Managing financial risk tradeoffs for hydropower generation using snowpack-based index contracts

Andrew L. Hamilton[1,2], Gregory W. Characklis[1,2], and Patrick M. Reed[3]

[1]Department of Environmental Sciences and Engineering, Gillings School of Global Public Health, University of North Carolina at Chapel Hill, Chapel Hill, NC, USA
[2]Center on Financial Risk in Environmental Systems, Gillings School of Global Public Health, UNC Institute for the Environment, University of North Carolina at Chapel Hill, Chapel Hill, NC, USA
[3]Department of Civil and Environmental Engineering, Cornell University, Ithaca, NY, USA

Key Points:

- A snowpack-based index contract is developed that hedges hydropower revenue variability for a producer in a snow-dominated system.
- Multi-objective optimization is used to explore financial tradeoffs for risk management portfolios of index contracts, reserves, and debt.
- A sensitivity analysis shows the utility's fixed cost burden is a critical factor in determining optimal management strategies and outcomes.

Corresponding author: Andrew L. Hamilton, andrew.hamilton@unc.edu

Abstract

Hydrologic variability poses an important source of financial risk for hydropower-reliant electric utilities, particularly in snow-dominated regions. Drought-related reductions in hydropower production can lead to decreased electricity sales or increased procurement costs to meet firm contractual obligations. This research contributes a methodology for characterizing the tradeoffs between cash flows and debt burden for alternative financial risk management portfolios, and applies it to a hydropower producer in the Sierra Nevada mountains (San Francisco Public Utilities Commission). A newly designed financial contract, based on a snow water equivalent depth (SWE) index, provides payouts to hydropower producers in dry years in return for the producers making payments in wet years. This contract, called a capped contract for differences (CFD), is found to significantly reduce cash flow volatility and is considered within a broader risk management portfolio that also includes reserve funds and debt issuance. Our results show that solutions relying primarily on a reserve fund can manage risk at low cost, but may require a utility to take on significant debt during severe droughts. More risk-averse utilities with less access to debt should combine a reserve fund with the proposed CFD instrument in order to better manage the financial losses associated with extreme droughts. Our results show that the optimal risk management strategies and resulting outcomes are strongly influenced by the utility's fixed cost burden and by CFD pricing, while interest rates are found to be less important. These results are broadly transferable to hydropower systems in snow-dominated regions facing significant revenue volatility.

1 Keywords

Hydropower, snow, drought, financial risk, decision support, uncertainty

2 Introduction

Hydrologic variability can significantly impact the financial stability of hydropower-producing electric utilities. During dry periods, independent hydropower producers selling into the wholesale market can suffer reduced revenues, while retail load-serving entities with firm obligations can see increased costs as they are forced to replace hydropower with more expensive thermal generation. This type of financial variability presents problems for many types of activity. Most firms take financial risk management actions to reduce volatility, which can be explained by their concerns over a number of factors: re-

duction of credit risk and cost of capital, reduction of the impact and likelihood of serious financial distress, and self-interest of risk-averse management (Bank & Wiesner, 2010; G. W. Brown & Toft, 2002; Froot, Scharfstein, & Stein, 1993). These issues may be even more pressing for public and regulated utilities, which are relatively constrained with respect to pricing and management options available during times of stress such as drought. Because their revenues are roughly proportional to electricity sales, while their costs (debt service, operations and maintenance, etc.) are largely fixed, hydropower-reliant power utilities are especially vulnerable to financial distress during drought. Credit ratings agencies such as Moody's Investors Service have cited drought conditions as a significant risk factor for power utilities with significant hydropower generating assets (Moody's Investors Service, 2019), and warn that such utilities should "ensure that power supply and financial margins can withstand low water periods; plan for replacement power and [financial] liquidity" (Moody's Investors Service, 2011).

In general, management of hydrologic financial risks can take the form of physical actions such as supply capacity expansion, water use reduction/recycling, or temporary water purchases, as well as financial actions such as self-insurance through a reserve fund, debt issuance, or financial hedging (Larson, Freedman, Passinsky, Grubb, & Adriaens, 2012). When evaluating the effectiveness of any given tool for reducing financial risk, it is important to consider its place within a larger risk management strategy. Like most businesses, a power utility will maintain a reserve fund in order to self-insure against some level of unexpected losses. The utility can deposit into this fund when revenues exceed costs (most likely in wet years for hydropower-reliant utilities), and withdraw from the fund when revenues are insufficient to cover expenditures (most likely in dry years). Additionally, they have the ability to issue debt (i.e., borrow money) to take up the slack when the reserve fund balance is insufficient to meet a cash flow deficit. Debt can take a variety of forms, but one common form is the issuance of debt in the commercial paper markets. Commercial paper is a type of short-term debt instrument, typically maturing in less than a year, which allows corporations to borrow money in order to cover short-term financial obligations such as accounts payable and payroll. A utility may use a Letter of Credit agreement, which allows it to issue commercial paper that is backed by a bank. This can assuage the credit concerns of lenders and lower the effective interest rate, even after paying a fee to the bank.

In addition to self-insurance and debt issuance, a utility can hedge in order to shift financial risk to another party more willing to hold that risk. Environmental index contracts, also known as weather derivatives, use environmental metrics (e.g., cumulative precipitation or temperature) to define contracts that provide payouts based on a predefined index measured at a specific time and place. For example, natural gas suppliers commonly purchase "temperature derivatives," which define payouts based on seasonal temperature indexes called heating and cooling degree days (Ellithorpe & Putnam, 2000; Jewson, Brix, & Ziehmann, 2005). In the event of an unusually warm winter (as measured by deviations from a heating degree day index benchmark), when demand for heating is below expectations and natural gas sales tend to lag, the contract would provide a payout that would reduce the impact of low revenues. Index contracts based on both precipitation and temperature have been studied extensively for hedging crop yield risk (Cyr & Kusy, 2007; Vedenov & Barnett, 2004; Woodward & García, 2008), and have also been applied in practice (Alderman & Haque, 2007; United States Department of Agriculture Risk Management Agency, 2017). Index contracts based on water level have been proposed for protection against shipping disruptions in the Great Lakes (Meyer, Characklis, Brown, & Moody, 2016), and metrics based on cumulative streamflow (C. Brown & Carriquiry, 2007; Zeff & Characklis, 2013) and the Palmer Hydrologic Drought Index (Baum, Characklis, & Serre, 2018) have been proposed for hedging hydrologic risk experienced by urban water utilities.

Hydrologic financial risk is present at all life stages of a hydropower plant, from financing to construction to operation (Blomfield & Plummer, 2014), but this work focuses on hydrologic financial risks to currently operating hydropower systems. A power utility reliant on hydropower faces two major types of financial risks: price risk associated with the value of power sold and/or purchased, and quantity risk associated with the quantity of power demanded by customers and the quantity of power produced. In deregulated electricity markets (e.g., California), the former can be hedged using options, forwards or futures contracts on the price of electricity and/or natural gas (Deng & Oren, 2006). The demand side of quantity risk can often be effectively hedged using temperature derivatives (Ellithorpe & Putnam, 2000; Jewson et al., 2005). However, the supply side of quantity risk, driven by hydrologic variability, can be much more difficult to manage. A portion of the supply risk can be hedged with power price derivatives by taking advantage of correlations between price and supply (Oum, Oren, & Deng, 2006), but

these tend to be be weakly related such that significant risk remains. However, hydrologic index contracts are a promising tool for hedging supply risk. Streamflow and water storage have both been suggested for hedging hydropower producers' drought risk (Denaro, Castelletti, Giuliani, & Characklis, 2018; Foster, Kern, & Characklis, 2015; Meyer, Characklis, & Brown, 2017).

This work proposes an index contract based on snow water equivalent depth (SWE). Although the Chicago Mercantile Exchange has developed contracts based on snowfall at select locations, used by municipalities and businesses such as snow removal companies and ski resorts (Chicago Mercantile Exchange Group, 2014; Nielsen, 2012), the authors are not aware of any academic literature quantifying the benefits of such an index for hydropower or other industries. Roughly one sixth of the global population, producing one fourth of the global GDP, is estimated to live in regions where water availability is predominantly influenced by snowmelt (Barnett, Adam, & Lettenmaier, 2005). In many regions, such as California's Sierra Nevada, snowpack functions as a reservoir by storing precipitation until the spring and summer melt period, and winter/spring SWE measurements are a critical tool for forecasting spring/summer runoff in these regions (Anghileri et al., 2016; Denaro, Anghileri, Giuliani, & Castelletti, 2017). A SWE index thus has a timing advantage over streamflow-based indices; the SWE index is available at the end of the snowfall season (generally taken as April 1 in California), while a streamflow-based index would not be calculable until the end of the snowmelt season (frequently lasting until July in California). Earlier availability of cash flows from the contract may allow managers to take further and more informed risk management actions, whether physical or financial, over the ensuing months.

Drought can be defined in a number of ways. "Meteorological drought" refers to a deficit of precipitation, while "agricultural drought" and "hydrological drought" refer to deficits of soil moisture and runoff, respectively. In this work, we will mainly refer to hydrological drought as it pertains to hydropower. Additionally, a "snow drought" refers to a deficit of snow accumulation, caused by low precipitation, high temperature, or a combination of the two (Gonzalez et al., 2018; Wehner, Arnold, Knutson, Kunkel, & LeGrande, 2017). California experienced an historic drought over the 2012-2016 period, caused by an extreme combination of low precipitation and high temperatures (AghaKouchak, Cheng, Mazdiyasni, & Farahmand, 2014; Diffenbaugh, Swain, & Touma, 2015). Negative impacts on the state's municipal water supplies, groundwater supplies, agri-

culture, forests, recreation, aquatic ecosystems, and water quality have been documented (Lund, Medellin-Azuara, Durand, & Stone, 2018). Another important impact is reduced hydropower generation. The majority of hydropower production in the state occurs at small, high-altitude reservoirs in the Sierra Nevada mountains with little carryover capacity, meaning that hydropower production is closely tied to annual snowmelt runoff in alpine watersheds. Consequently, the percentage of California's power mix from hydropower was only 5.4% in 2015, at the height of the drought, compared to 14.7% in 2017, a year with significantly more precipitation (California Energy Commission, 2018). The hydropower deficit over the five-year drought, largely replaced by more expensive power from natural gas turbines, cost the state an estimated $2.45 billion, as well as a 10% increase in greenhouse gas emissions (Gleick, 2017).

The overarching goal of this research is to develop a methodology for discovering optimal financial risk management strategies for hydropower producers in snow-dominated systems. Each risk management portfolio consists of some combination of a reserve fund, an ability to issue short-term debt, and a novel SWE-based index contract called a capped contract for differences (CFD). A stochastic financial simulation model is embedded within a multi-objective optimization in order to explore the tradeoffs between an expected annualized cash flow objective and a 95th percentile maximum debt objective. Lastly, we contribute a unique sensitivity analysis, in which the multi-objective optimization is repeated for alternative states of the world (SOWs) attained using a global Latin Hypercube sampling of five financial parameters that depend on the context of the utility: the ratio of the utility's fixed costs to its average hydropower revenues, the market price of risk for the CFD, the real discount rate, and the real interest rates governing the reserve fund and debt. Optimizing across the alternative SOWs explicitly shows how the set of optimal financial risk management strategies, as well as the resulting set of tradeoffs between the cash flow and debt objectives, changes as a function of these key contextual parameters. The methodology is demonstrated using a case study based on the San Francisco Public Utilities Commission's Power Enterprise, which produces hydropower in California's central Sierra Nevada. However, these results provide financial risk management insights broadly for power producers with significant hydropower resources, particularly those in snow dominated systems.

3 Methods

3.1 Study Area

Hetch Hetchy Power Enterprise is the electricity division of San Francisco Public Utilities Commission (SFPUC). SFPUC operates three reservoirs in the headwaters of the Tuolumne River in the central Sierra Nevada: Hetch Hetchy Reservoir, Cherry Lake and Lake Eleanor. Inflow to these reservoirs, primarily driven by the seasonal dynamics of snow accumulation and melt, drives hydropower turbines at the Holm, Kirkwood, Moccasin, and Moccasin Low-Head Powerhouses. This power is sold at fixed rates via firm contracts to customers such as the San Francisco International Airport, municipal buildings in San Francisco, and a small number of other retail customer classes. Modesto and Turlock Irrigation Districts have the option to buy surplus power at a lower fixed rate, as stipulated in the Raker Act that authorized the construction of Hetch Hetchy Reservoir. Additionally, SFPUC buys and sells wholesale power on the Western Systems Power Pool (San Francisco Public Utilities Commission, 2016).

3.2 Data Sources

Monthly observations of snow water equivalent depth (SWE) for Dana Meadows, the snow station upstream of the hydropower-producing reservoirs with the longest record (64 years), is available from the California Data Exchange Center's online database (California Data Exchange Center, 2018). The monthly observations for February and April, typically performed within one week of the first day of the stated month, will be referred to as February 1 and April 1 measurements. Observations from months other than February and April are also available, but as the records are shorter and less consistent, they are not used in this study. Hydropower generation data are provided by SFPUC Power Enterprise (San Francisco Public Utilities Commission, 2018). Volumetrically-weighted average daily spot peak prices on the Northern California NP-15 electricity hub are available from the US Energy Information Administration (United States Energy Information Administration, 2017). Historical retail electricity rates and sales data are taken from the 2015-2016 SFPUC financial statement (San Francisco Public Utilities Commission, 2016).

3.3 Modeling Framework

The multi-level framework used in this research is outlined in Figure 1. The innermost level consists of the financial simulation model, which simulates the financial operations of the utility over a 20-year period. The inputs to the simulation model are a 20-year sample of the stochastic drivers, an operating policy, and a state-of-the-world (SOW), defined as a combination of five contextual financial parameters (ratio of fixed costs to average revenues, pricing parameter for the CFD, real discount rate, and real interest rates for the reserve fund and debt). As seen in Figure 2, the financial simulation model uses these inputs to perform a cascade of financial operations (on an annual time step) that updates variables such as the hydropower revenue, capped contract for differences (CFD) net payout, reserve fund balance, debt, and final cash flow. These variables are described in Sections 3.5, 3.6, and 3.7. The 20-year time horizon is chosen to be long enough to capture the internal variability of the reserve fund balance and the debt load. These state variables can dynamically rise and fall over a period of multiple years based on sequences of high or low snowfall and/or power price, so it is important to test each risk management strategy on multi-year sequences rather than single years in isolation.

As seen in Figure 1, this 20-year financial simulation model is embedded within a Monte Carlo evaluation level in order to account for the inherent variability of the stochastic drivers (snow water equivalent depth (SWE), hydropower generation, and wholesale power price). An ensemble of 50,000 samples is generated (Section 3.4), and each 20-year sample is run through the financial simulation model. The results from the members of the ensemble are aggregated to calculate the dual objectives of expected annualized cash flow (to be maximized) and 95th percentile maximum debt load (to be minimized), as well as a constraint that ensures debt use is sustainable (Section 3.8).

Each Monte Carlo evaluation is carried out subject to a fixed operating policy, defined as a slope for the CFD (in $M/inch SWE) and a maximum reserve fund balance. In the next level of the workflow in Figure 1, the ensemble objectives and constraint are used to optimize the operating policy using the Borg Multi-Objective Evolutionary Algorithm (MOEA). Because tradeoffs exist between the multiple objectives, the output of a multi-objective optimization (MOO) is a set of non-dominated solutions, rather than a single optimal solution. During the search, the Borg MOEA uses evolutionary heuris-

tic strategies to generate many candidate policies, each of which is evaluated based on its multi-objective performance on the Monte Carlo evaluation. This process is elaborated upon in Section 3.8.

Lastly, the process is embedded within a sensitivity analysis (Figure 1), in which the MOO is repeated for many different states of the world (Section 3.9). Each state of the world (SOW) is defined by the values of five contextual financial parameters: the ratio of fixed costs to average revenues, the pricing parameter for the CFD, the real discount rate, and the real interest rates for the reserve fund and debt. A typical sensitivity analysis in an applied optimization study is situated "downstream" of the optimization, in that it proceeds in the following order: (1) Assume a SOW; (2) Optimize the system as if the assumed SOW is true; (3) Test the sensitivity of solutions by sampling alternative SOWs and recalculating performance of the solutions within the new SOWs. The sensitivity analysis employed in this study, on the other hand, can be thought of as "upstream" of the optimization and proceeds in the following order: (1) Sample alternative SOWs; (2) For each, optimize the system under the assumed SOW; (3) Explore the differences in the optimal solutions themselves, as well as differences in attainable performance, across SOWs. In other words, the downstream sensitivity analysis is concerned primarily with uncertainty, and answers the questions, "What if we design and implement an irreversible plan, and we are wrong about our assumptions? How bad can it be?" The upstream sensitivity analysis used in this study, on the other hand, is primarily interested in contextual differences rather than uncertainty, and answers the questions, "How important are contextual factors, with known values at decision-making time, in determining which operating policies are best? How do these factors affect a decision-maker's attainable performance and perceived tradeoffs between objectives?"

3.4 Synthetic Data

The main stochastic drivers are the snow water equivalent depth (SWE), hydropower generation, and the wholesale power price. In order to adequately gauge risk, it is desirable to have a larger sample of potential outcomes than can be found in the historical record. For this reason, the statistical properties of historical time series are used to generate a million-year synthetic time series for SWE (Section 3.4.1), hydropower generation (Section 3.4.2), and power price (Section 3.4.3). The synthetic SWE and hydropower records are generated concurrently to mimic their historical correlations, but power prices

are assumed to be independent (see Section 4.4). For the Monte Carlo evaluation (Figure 1), a 50,000-member ensemble of 20-year samples is taken from this million-year record.

3.4.1 Synthetic Snow Water Equivalent

Both February 1 and April 1 SWE measurements are available for each year 1952-2016, except 1963, a total of 64 years. The historical snow water equivalent (SWE) record is not found to exhibit any statistically significant trend or autocorrelation at an annual time step. Both February 1 and April 1 SWE observations are fit to a gamma distribution, passing a Kolmogorov-Smirnov test of goodness of fit. These gamma distributions are linked using a Gaussian copula (Frees & Valdez, 1998; Genest & Favre, 2007; Genest, Favre, Béliveau, & Jacques, 2007; Sklar, 1973; Wang, 1999) in order to generate synthetic February 1 and April 1 SWE observations that preserve the historical Kendall's rank correlation. As seen in Figure 3 (top left), the synthetic dataset matches the statistical properties of the historical data, while providing a broader array of potential outcomes for risk assessment. Additional details on methods and parameter estimates can be found in Supporting Information Section S1.

3.4.2 Synthetic Hydropower Generation

Total generation for the water year (October-September) is aggregated to a monthly time step. Due to the dominance of winter precipitation and spring snowmelt in Sierra Nevada hydrographs, hydropower production at high alpine reservoirs is highly seasonal, peaking in spring and early summer. In order to capture the relationship between snowpack and monthly generation, separate predictors are developed for each month of the water year, using the 29 water years available, 1988-2016.

Hydropower generation for each month is estimated using one of three models: (1) constant (independent of SWE), (2) linearly increasing in SWE, and (3) linearly increasing in SWE up to a threshold, beyond which expected generation is flat. This third piecewise model is necessary in the peak snowmelt period of March through June, and reflects the fact that in the wettest years, some water may need to be spilled without generating hydropower. Readers interested in additional modeling details and parameter estimates are referred to Supporting Information S2.

After estimating a model for each month, each historical observation from water year y and month m is converted to a model residual, $r_{m,y}$. Residuals for the constant and linear models are deseasonalized by calculating monthly z-scores, as $\tilde{r}_{m,y} = (r_{m,y} - \mu^r_m)/\sigma^r_m$, where μ^r_m and σ^r_m are the mean and standard deviation of all residuals from month m. For the piecewise models (March-June), observations with SWE above the threshold are separated from those below the threshold. The deseasonalization is then performed separately for each group, in order to account for the fact that residual variability is much lower for the wet years above the piecewise threshold (see Figure S2 in Supporting Information). The time series of deseasonalized residuals is found to exhibit significant monthly autocorrelation and is fit to an autoregressive (AR) model with significant lags at one month and three months. The residuals from the AR model are not found to exhibit significant autocorrelation and are not found to deviate significantly from a normal distribution. Additional details and parameter estimates for the AR model can be found in Supporting Information Section S2.

This process is reversed to create a synthetic time series of monthly hydropower generation that is consistent with the synthetic SWE record. This involves sampling from a normal distribution with the same variance as the residuals from the AR model, in order to get synthetic residuals. These are run through the autoregressive model, reseasonalized based on month and SWE, and added to the (piecewise) linear predictions based on month and SWE. The historical minimum and maximum monthly generation (17.81 and 256.27 GWh/month, respectively) are used to bound the synthetic observations, under the assumption that these represent system constraints.

Figures 3 (bottom left) and 4 (top) suggest that the historical relationships between hydropower generation, SWE, and month are well represented in the synthetic data. It is also apparent from Figure 3 (bottom left) that the synthetic dataset provides a broader array of potential outcomes for risk assessment, including both more and less productive years for hydropower than are present in the historical record. Spearman's rank correlation coefficient between SWE and annual hydropower generation is 0.894, confirming that SWE is a dominant driver of hydropower production. However, hydropower generation tends to level off in very wet years, as operational capacity constraints are reached. This effect is noticeable in Figure 3 (bottom left) as well as Figure 4 (top), where hydropower appears to reach capacity in wet years between March and June.

3.4.3 Synthetic Wholesale Power Prices

Daily wholesale power price data for the seven water years 2010-2016 are averaged to a monthly time step and inflated to October 2016 dollars using historical inflation rates based on the Consumer Price Index (Bureau of Labor Statistics, 2019). Prices are then log-transformed and deseasonalized by calculating z-scores within each month of the year, as $\tilde{p}_{m,y} = (p_{m,y} - \mu^p_m)/\sigma^p_m$, where $p_{m,y}$ is the log power price for month m in year y, and μ^p_m and σ^p_m are the mean and standard deviation of all log prices for each month m. Next, the deseasonalized log prices are fit to a seasonal autoregressive moving average (SARMA) model consisting of a single lag of one month for the autoregressive model, plus a moving average error model with a single lag of twelve months. The residuals from the SARMA model are not found to exhibit significant autocorrelation and are not found to deviate significantly from a normal distribution. Additional details and parameter estimates can be found in Supporting Information S3.

Following model specification, a synthetic record is created by sampling from a normal distribution for the residuals, running these residuals through the SARMA model, and reseasonalizing based on month. This gives synthetic log-prices, which are exponentiated to produce monthly average power prices in October 2016 dollars. Figure 4 (bottom) suggests that the historical relationship between power price and month is well represented in the synthetic data. However, one limitation is that the relationship between hydrology and power price over the entire electricity market has not been modeled, as will be discussed in Section 4.4.

3.5 Revenue Model

The revenue model considered in this paper is based on the operations of SFPUC's power enterprise (San Francisco Public Utilities Commission, 2015, 2016). The utility sells power to three major classes of customer. First, the utility must satisfy the demand from its retail customer base, made up of the San Francisco International Airport, government buildings in San Francisco, and a limited number of other retail customer classes. This power is sold at a fixed rate that is generally higher than the wholesale price of power. If hydropower generation is insufficient to meet this demand, the utility must purchase power on the wholesale market, at the variable market rate, to make up the difference.

In the event that hydropower generation is in excess of retail demand, the Modesto and Turlock Irrigation Districts (MTID) are granted the option to purchase a portion of this surplus power at fixed rates that are generally lower than wholesale power prices. In the event that wholesale prices fall below this fixed rate, we assume that MTID will opt to purchase power from the wholesale market rather than the utility. Lastly, any hydropower generation in excess of retail and MTID demand is sold on the wholesale market at the variable market rate.

Given synthetic time series of hydropower generation and wholesale power prices, this model can be used to simulate the resulting revenues ("Hydropower revenues" in Figure 2). For simplicity, in this paper the term "revenue" will be used to refer to the net effect of hydropower sales minus wholesale power purchases. All revenues are reported in October 2016 dollars. Readers are directed to the Supporting Information Section S4 for additional details on the revenue model.

Lastly, power utilities are capital-intensive enterprises that can typically be expected to have large costs from debt service, operations and maintenance, capital expenditures, and salaries (Moody's Investors Service, 2011; San Francisco Public Utilities Commission, 2016). These costs in general must be met each year, regardless of how much hydropower is produced, and can be considered constant on the time scale of a typical drought. Fixed costs as a fraction of average revenues are estimated from SFPUC's financial statements as the average of (operating expenses minus power purchases) divided by (operating revenues minus power purchases) over the 2010-2016 period (San Francisco Public Utilities Commission, 2016), yielding 0.914. Fixed costs are thus assumed to be 91.4% of the mean revenue, as calculated over the 1,000,000 synthetic years. Net revenues (Figure 2), or revenues minus fixed costs, are positive when revenues are sufficient to cover fixed costs, and negative otherwise. A sensitivity analysis is also performed (Section 3.9) in order to gauge the impact of the fixed cost fraction on the set of optimal operating policies and the resulting financial performance of the utility.

The correlation between annual hydropower revenue and SWE can be seen in Figure 3 (right). Spearman's rank correlation coefficient is found to be 0.859 for the synthetic dataset. Much like hydropower generation, revenues are roughly linearly related to SWE, except for very wet years, in which revenues start to level off due to operational capacity constraints on hydropower production. The variance of revenues is seen to in-

crease at high SWE values as well, where a larger proportion of power is sold as surplus in the wholesale market at variable rates. Also shown in Figure 3 (right) is a pseudo-historical dataset generated by running the 29 years of historical hydropower generation (same as in bottom left plot) through the revenue model with a randomly-selected 29-year long sequence of synthetic power prices. This cannot be used as a direct comparison to SFPUC's actual revenues for validation, due to changing customer base, retail rates, and power prices over this period. However, it does still highlight the benefit of the synthetic hydropower generation dataset, which helps to generate a broader distribution of potential revenues than the historical hydropower generation dataset allows.

3.6 Index Contract

When designing any index contract, the first step is to specify an index that is highly correlated with a financial variable of interest (such as revenues) over a designated time period. The correlation between snowpack and hydropower revenue suggests that hydrologic financial risk could be hedged using a snowpack-based index contract. Next, the functional relationship between the index and contract payouts must be specified. The last step is then to price the contract.

3.6.1 Index Development

In the Sierra Nevada, the April 1 SWE measurement is often used in management decisions as a proxy for annual peak SWE. Consequently, April 1 SWE would be a logical index around which to base a contract. However, as described in Section 3.4.2, both February 1 and April 1 SWE are important for estimating SFPUC annual hydropower generation. April 1 SWE is indeed the strongest predictor of generation in the months of February through June, but February 1 SWE is a better predictor for November, December and January generation. In years when snowfall is concentrated either before or after February 1, it is important to account for the effect of this timing on hydropower production. For this reason, we use the following weighted average of February 1 and April 1 SWE for the contract index:

$$Index = 0.3122 S_F + 0.6878 S_A \tag{1}$$

The weights for this average are taken from the normalized coefficients of a linear regression mapping February 1 and April 1 SWE to total power revenues over the water year.

When designing any index contract, "basis risk" is a concern. Basis risk represents the risk that the contract buyer will not receive a payout when losses occur, or will receive a payout when losses do not occur. This risk arises due to the uncertainty in the index-revenue relationship, because the correlation between the index and revenue is never perfect (Woodward & García, 2008). The basis risk in this case arises from a combination of wholesale power price variability, error from using snow station point measurements as a proxy for total-watershed SWE, and variability in hydrologic factors such as evaporation and melt timing. A number of other potential indices were considered for this study, including aggregated measures of total precipitation or streamflow. The weighted SWE index is chosen due to its high correlation with hydropower generation and its long historical record. Techniques such as interpolation, remote sensing, modeling, and reanalysis could be used to develop indices in regions with more sparse ground measurements (Margulis, Cortés, Girotto, & Durand, 2016; Wrzesien et al., 2017; Zheng, Molotch, Oroza, Conklin, & Bales, 2018). However, ground measurements, when they exist, have the advantages of being simple, transparent, and immediately available.

3.6.2 Contract Structure

After establishing an index, the next step in contract design is to choose the contract structure. The contract should provide payouts to the utility in years of financial distress, which in this case is defined as low revenues arising from drought. A variety of contract structures exist, but this work focuses on a "capped contract for differences", which is found to effectively hedge risk in the current context. This contract structure and closely related structures are variously referred to as forward contracts, futures contracts, and swap contracts in the weather derivatives literature (Chicago Mercantile Exchange Group, 2014; Hull, 2009; Jewson et al., 2005), but we will use the contract for differences (CFD) terminology for its conceptual clarity.

Under the proposed CFD, the utility and the contract seller agree to settle the difference between the eventual value taken by the SWE index and some predefined reference value. As portrayed in Figure 5, the utility would receive positive net payouts when the SWE index falls below the reference value, and negative net payouts (i.e., they would owe payments) when the index falls above the reference value. Additionally, negative net payouts are capped at the 95th percentile of the SWE distribution (48.44 inches). The net effect is that the buyer of the contract will receive payouts in dry years, when they

expect to have hydropower revenue shortfalls. In return, they make payments to the contract seller in years of high SWE, when the utility expects to have ample hydropower revenues. This allows the utility to sell its upside in order to finance its downside protection. The intent of the cap is to limit payments by the utility in exceptionally wet years, when the index-revenue relationship tends to break down due to operational limits on hydropower production.

The slope of the CFD, in units of dollars per inch of SWE, can be tailored to fit the risk profile of the utility. This slope is often set by regressing the financial metric (e.g., annual net revenues) against the index. However, this may not be the best strategy if the regression residuals display non-normality or heteroscedasticity. Other authors have used quantile regression, variance or semi-variance minimization, or other methods in order to more effectively hedge the impact of extreme events (Conradt, Finger, & Bokusheva, 2015; Manfredo & Richards, 2009; Vedenov & Barnett, 2004). In this study, the contract slope is set within a multi-objective optimization, as explained in Section 3.8. This allows for the optimal hedging policy to be determined within the broader context of an integrated risk management portfolio.

The proposed contract is assumed to have a six-month duration. The parties enter into the contract at the beginning of the water year, October 1, before snow typically begins to accumulate and when little predictive power regarding the winter snowpack exists (Kapnick et al., 2018; Shukla & Lettenmaier, 2011). The net payout is settled after observing the February 1 and April 1 SWE. In practice, the purchaser of a CFD might be required to pay a discounted premium or margin up front, but we assume for simplicity that the net payout is settled after the April observation.

3.6.3 Contract Pricing

The reference value of the SWE index, which determines the boundary between positive and negative net payouts, is determined by a contract pricing process. In finance, derivative contracts are typically priced using the Black-Scholes formula or one of its many extensions (Black & Scholes, 1973; Hull, 2009). These prices are relatively transparent and well-behaved due to no-arbitrage assumptions, as long as both the derivative contract and the underlying product are traded at sufficiently high volumes. However, pricing environmental index contracts is more difficult, because the underlying index (e.g.,

SWE) is not a tradable commodity. The Chicago Mercantile Exchange does provide exchange-traded contracts on temperature and other weather variables, including monthly snowfall at a small number of locations (Chicago Mercantile Exchange Group, 2007, 2014), but the majority of weather index contracts are traded over-the-counter in private transactions, meaning that prices are typically not publicly-available. Additionally, because contracts tend to be tailored to specific local circumstances, prices may not be generalizable. For these reasons, the pricing of weather index contracts is less straightforward than derivative contracts indexed on interest rates, stocks, or oil.

A number of actuarial methods exist for estimating the price of environmental index contracts, or equivalently, the reference value for a CFD. The "actuarially-fair" way is to set the reference value such that the expected value of the contract is zero (i.e., expected value of positive payouts is equal to expected value of negative payouts). However, the party selling the contract typically subtracts a "loading" from the contract, so that the expected value of the contract is negative for the buyer (e.g., the utility) and positive for the contract seller. In other words,

$$X(s) = \tilde{X}(s) - loading \tag{2}$$

where s is the observed value of the SWE index, $\tilde{X}(s)$ is the actuarially-fair net payout function ("No loading" in Figure 5), and $X(s)$ is the net payout function after accounting for the loading applied by the contract seller (e.g., "Baseline loading" or "High loading" in Figure 5).

The loading represents the sum of administrative costs, expected profit, and "risk loading." The risk loading is an additional amount required to take on more risk. Because the contract seller may need to make large payouts in the future, they must maintain adequate liquid reserves. Liquid reserves have an opportunity cost, as these reserves could earn a higher rate (even while maintaining a similar level of risk) if invested in a less liquid fashion. A contract with more variable payouts, such as those resulting from low frequency, high magnitude events, will thus have a larger risk loading because the seller of the contract will be required to maintain large, infrequently used reserves, and will expect to be compensated for the opportunity cost of maintaining such reserves. For this reason, actuarial "premium principles" are often used, which price contracts using formulas that rely on the expected value of payouts as well as the probability of more extreme events (Jewson et al., 2005; Young, 2004).

The method used in this study is the Wang Transform (Wang, 2002), which transforms the probability distribution of payouts into a risk-adjusted distribution in which more extreme payouts are weighted more heavily, written:

$$F^*(x) = \Phi[\Phi^{-1}(F(x)) + \lambda] \tag{3}$$

where $F(x)$ is the original cumulative probability distribution function (cdf) of payouts x, $F^*(x)$ is the risk-adjusted cdf, and λ is the "market price of risk" determining the size of the risk premium demanded by contract sellers. For more details on the numerical implementation of this method, see Supporting Information Section S5.

Following other work on weather derivative contracts (Baum et al., 2018; Foster et al., 2015; Wang, 2002), $\lambda = 0.25$ ("Baseline loading" in Figure 5) is used as the baseline value for pricing the contract in this study. However, values between 0 ("No loading") and 0.5 ("High loading") are included in the sensitivity analysis, as described in Section 3.9. The no-loading scenario has the highest SWE reference value, where the net payout function intersects zero. This is the most favorable scenario for the utility, as it has the highest chance of positive payouts and the highest expected value. The high loading scenario has the opposite effect, with a lower SWE reference value and a correspondingly lower expected value. For example, assuming a contract slope of \$1 million per inch of SWE, the reference value for the baseline loading scenario is 24.71 inches, approximately the 51th percentile. With no loading, the payout structure and reference value shift upwards by \$1.19 million and 1.19 inches, respectively. With high loading, on the other hand, the payout structure and reference value shift downwards by \$1.34 million and 1.34 inches, respectively.

A final note on pricing: the ability to forecast winter snowfall in the Central Sierra Nevada is relatively poor prior to the beginning of the water year on October 1 (Kapnick et al., 2018; Shukla & Lettenmaier, 2011). For this reason, it is reasonable to assume that the expected payout for any given contract does not change from year to year based on October 1 conditions. However, in the event that forecasting improves in the future, one of two actions would need to be taken: either the parties would enter into the contract earlier in the year at a date with negligible forecasting skill, or else forecasts would be incorporated into a conditional probability distribution for SWE on October 1, which would be used to adjust the contract premium each year. If contract premiums were not adjusted to reflect the forecasts, customers would only enter into contracts in

549 years in which they expected positive net payouts, resulting in an intertemporal adverse
550 selection and large financial losses for the contract seller (Carriquiry & Osgood, 2012;
551 Nadolnyak & Vedenov, 2013).

552 3.7 Reserve Fund and Debt Issuance

553 When evaluating the effectiveness of index contracts for hedging financial risk, it
554 is important to place them within a larger risk management strategy. Like most busi-
555 nesses, power utilities typically maintain a reserve fund in order to self-insure against
556 some level of unexpected losses. Additionally, they have the ability to issue short-term
557 debt (i.e., borrow money) in the event of short-term cash flow problems.

558 Cash available at the end of the water year before any financial operations ("Cash
559 before WD" in Figure 2, where WD stands for withdrawal) is equal to net revenue (hy-
560 dropower revenue minus fixed costs), plus the net payout of the capped contract for dif-
561 ferences (CFD). Reserve fund withdrawals are then used to make up for cash flow deficits
562 (i.e., "Cash before WD" < 0) when possible. When cash flow surpluses (i.e., "Cash be-
563 fore WD" > 0) exist, the utility makes deposits into the reserve fund. In Figure 2, the
564 "Withdrawal (WD)" box can represent either a withdrawal (WD > 0) or a deposit (WD
565 < 0). A limit on the reserve fund balance ("Max fund") is set within the multi-objective
566 optimization (Section 3.8), so that positive cash flows can be realized once the reserve
567 fund has reached capacity. The reserve fund is assumed to be invested in a safe and liq-
568 uid form, such as money markets, and earn a return of I_F% per year.

569 In years when the reserve fund is insufficient to cover the cash flow deficit (i.e. "Cash
570 after WD" < 0), the utility is assumed to issue short-term debt to cover the difference.
571 This debt could take a variety of forms, such as a Letter of Credit (LOC) agreement with
572 a large bank, which would allow the utility to issue commercial paper that is backed by
573 the bank. This would allow them to borrow money at a lower rate than could be achieved
574 without the LOC (e.g., by taking out a loan), in exchange for a fee paid to the bank. This
575 debt, plus interest of I_D after correcting for inflation, is assumed to be paid back the fol-
576 lowing year ("Debt due" in Figure 2) and is subtracted from the following year's rev-
577 enues prior to the withdrawal step.

578 Thus, the "Final cash flow" at the end of the water year is equal to hydropower
579 revenues, minus fixed costs, minus last year's debt with interest, plus the SWE contract

net payout, plus (minus) the reserve fund withdrawal (deposit), and plus new debt. This final cash flow will be strictly non-negative, as debt issuance is assumed to take up the slack when other risk management tools are insufficient to ensure non-negative cash flow.

All interest rates are considered net of inflation so that all monetary values are reported in October 2016 dollars. The annual inflation estimate as of October 2016 is 1.6% (Bureau of Labor Statistics, 2019), and the annual return in Vanguard's Federal Money Market Fund between the fourth quarter of 2015 and the third quarter of 2016 is 0.25% (The Vanguard Group, 2019), yielding an inflation-adjusted interest rate on reserve funds of $I_F = -1.33\%$ per year. The negative interest rate implies that the money held in the reserve fund is not growing fast enough to keep up with inflation, which is common after fees in safe and liquid investments such as money markets. The interest rate paid on the debt, including the fee on the Letter of Credit, would vary depending on a number of factors, such as the utility's credit rating, the bank's size, and demand for debt in the financial markets. In this work, a rate of 1.4% per year above inflation is assumed, and both I_F and I_D are included in the sensitivity analysis in Section 3.9.

3.8 Objectives and Optimization

As seen in Figure 2, there are two degrees of freedom in the financial risk management policy taken by the utility: the SWE contract slope (in \$/inch), which affects the contract net payout each year) and the reserve fund limit (in \$, which affects withdrawals from and deposits to the fund). These two parameters are used as decision variables within the multi-objective evolutionary optimization. The minimum allowable SWE contract slope and reserve fund limit are set to \$50,000/inch and \$50,000, respectively, so that decision variables lower than these values are set to zero within the simulation. The optimization is carried out with respect to two conflicting objectives. The first is the expected annualized cash flow, which is to be maximized:

$$J^{cash} = E_N \left[\frac{1}{\sum_{y=1}^{Y} d^y} \left(\sum_{y=1}^{Y} \left(d^y C(n,y) \right) + d^{Y+1} \left((1+I_F)F(n,Y) - (1+I_D)D(n,Y) \right) \right) \right] \tag{4}$$

where $C(n,y)$ is the final cash flow at the end of year y of simulation n, after accounting for fixed costs, SWE contract net payouts, reserve fund withdrawals and deposits, new debt in year y, and debt plus accumulated interest from year $y-1$. $F(n,Y)$ and $D(n,Y)$ are the reserve fund balance and debt, respectively, at the end of the final year

of the simulation. The discount factor d is calculated from the real discount rate, δ, as $d = 1/(1+\delta)$. In Equation 4, the expression inside the outer brackets converts the variable cash flows over the $Y = 20$ years into a fixed annuity (\$/year) with equivalent present value. This is the "simulation objective" in Figure 1. The expectation operator E_N (the "ensemble aggregator") takes the mean over the N =50,000 Monte Carlo simulations to convert it into an "ensemble objective".

The real discount rate in J^{cash} accounts for the time value of money, and is set using the 20-year Treasury rate as of October 3, 2016, of 2.01% per year (United States Department of the Treasury, 2019). This is an approximately risk-free investment that reflects the opportunity cost of delaying cash flows into the future. Because all monetary values in this work are reported in October 2016 dollars, the discount rate is converted to a real rate by dividing out inflation of 1.6%, yielding a real discount rate of 0.40% per year for δ.

The second objective gives the 95th percentile of the maximum debt over 20 years:

$$J^{debt} = Q95_N[\max_Y[D(n, y)]] \tag{5}$$

where the $\max_Y$ operator takes the maximum value of the debt $D(n, y)$ over the years y within a given simulation (the simulation objective), while the $Q95$ operator takes the 95th percentile over the Monte Carlo samples n (the ensemble objective). This objective is minimized.

The following constraint is also applied to the simulated debt:

$$E_N\left[D(n, Y) - D(n, Y-1)\right] < \varepsilon \tag{6}$$

This constrains debt use to be sustainable, defined as growing (on average) by less than some ε. This ensures that the utility cannot borrow more and more every year with no hope of paying it back, which would likely land them in a credit crisis in practice.

A tradeoff is expected between the annualized cash flow objective J^{cash} and the maximum debt objective J^{debt}, so that there will not be a single optimal solution, but rather a Pareto-optimal set of solutions where improvement in one objective comes at the cost of degrading performance in the other conflicting objective. Plotting the Pareto-optimal set of policies in the objective space yields the Pareto frontier or optimal tradeoff that can inform decision makers' preferences. We solve the two-objective formulation presented in Equations 4-6 using a Multi-Objective Evolutionary Algorithm (MOEA).

MOEAs are a class of multi-objective optimization algorithms (for a detailed review, see Coello Coello, Lamont, and Van Veldhuizen (2007)) that have gained popularity in the fields of environmental and water resources systems due to their ability to solve difficult problems with properties such as nonlinearity, stochasticity, discreteness, non-convexity, high dimensionality, and uncertainty (Maier et al., 2014; Nicklow et al., 2010; Reed, Hadka, Herman, Kasprzyk, & Kollat, 2013). MOEAs use a variety of heuristic operators to iteratively improve a population of solutions with respect to multiple objectives. The Borg MOEA, the algorithm used in this study, has proven particularly adept across a wide range of problem types, and requires minimal problem-specific parameterization due to its adaptive operator selection (Hadka & Reed, 2013).

Each function evaluation (a trial of a new candidate policy) consists of a 50,000-member ensemble of 20-year simulations, resulting in a value for each of the two ensemble objectives, J^{cash} and J^{debt}, as well as a boolean value for the sustainable debt constraint. Each optimization run consists of 10,000 function evaluations. Due to the stochastic nature of evolutionary algorithms, each optimization is run multiple times; the baseline SOW is run with 50 seeds and each of the 150 additional SOWs in the sensitivity analysis are run with 10 seeds (the SOWs will be described in the next section). All seeds are found to converge quickly and produce very similar results (Figure S4-S6 in Supporting Information), as measured by the hypervolume, generational distance, and epsilon indicator metrics, which are commonly used to quantify convergence, diversity, and consistency in multi-objective optimization (MOO) (Coello Coello et al., 2007; Reed et al., 2013). After running the Borg MOEA for multiple seeds for each parameter sample, the best reference set is assembled for each parameter sample from among all of the candidate solutions. Each best reference set is then rerun on a second 50,000-member ensemble of 20-year simulations, and all results are reported for this test ensemble.

The ϵ-dominance parameters for J^{cash} and J^{debt} are set to \$75,000 and \$225,000, respectively. The debt sustainability constraint (ε in Equation 6) is set to \$50,000. These values, as well as the number of samples per function evaluation (50,000), are set in such a way that the variability in objective and constraint values across separate 50,000-member ensembles are generally smaller than the epsilon parameters. A large number of samples is needed per function evaluation, compared to other similar studies (e.g., (Quinn, Reed, Giuliani, & Castelletti, 2017)), due to the large internal variability relative to the desired error tolerance. This is partially attributable to the fact that the J^{debt} objective

definition leads to an extreme value distribution. All of the other Borg MOEA parameters are set using their default values as described in prior studies (Hadka & Reed, 2013). The uncertain or "noisy" MOO problem formulated here builds off of the recommendations of prior work for balancing computational demands and the fidelity of the forward Monte Carlo objective evaluations (see discussions in (Kasprzyk, Reed, Characklis, & Kirsch, 2012; Quinn et al., 2017; Zatarain Salazar, Reed, Quinn, Giuliani, & Castelletti, 2017)).

3.9 Sensitivity Analysis

The last step of the methodology, as illustrated in Figure 1, is the sensitivity analysis. The state of the world (SOW) is defined by the values of five contextual financial parameters: the ratio of the utility's fixed costs to its average hydropower revenues, the market price of risk for the CFD, the real discount rate for the annualized revenue objective, and the real interest rates for the reserve fund and debt issuance. These are contextual because they will vary both across decision-makers (e.g., the fixed cost ratio will vary significantly across different utilities) and across time (e.g., the interest rates will fluctuate with prevailing market forces). Note that the contextual parameters defining the SOW are distinct from the stochastic ensemble used in the Monte Carlo evaluation (SWE, hydropower generation, and power prices), which is assumed to vary with "well-characterized uncertainty" that is fixed across SOWs.

The MOO is first performed for a baseline SOW using parameter values estimated for SFPUC circa October 2016, as seen in Table 1. Derivation of estimates for the fixed cost fraction ($c = 0.914$), real discount rate (δ=0.40%), and market price of risk ($\lambda = 0.25$) can be found in Sections 3.5, 3.8, and 3.6.2, respectively. Estimates for the real interest rates on reserve funds ($I_F = -1.33\%$) and debt ($I_D = 1.4\%$) are given in Section 3.7. Because the discount rate is derived from the 20-year Treasury rate, which is strongly correlated with market-wide interest rates, the interest rates on reserve funds and debt are converted to relative rates (markdowns/markups from the discount rate) prior to sampling, by subtracting $\delta = 0.40$, and denoted by $\Delta_F = -1.73\%$ and $\Delta_D = 1.0\%$.

The sensitivity analysis makes use of 150 alternative SOWs from across the parameter ranges shown in Table 1. The SOWs are drawn from a global Latin hypercube sam-

ple, using the MOEA Framework software package (Hadka, 2015). Each SOW, consisting of a value for each of the five financial parameters, is used within a separate MOO, as seen in Figure 1. This allows us to test how the Pareto set of optimal risk management policies, and the attainable performance and tradeoffs between the cash flow and debt objectives, change as a result of the contextual parameters. The MOO for each SOW uses the same tuning parameters, seeds, and training/test ensembles of stochastic drivers, as described in Section 3.8.

4 Results and Discussion

4.1 Performance of Index Contract

As discussed in Section 3.6.2, the capped contract for differences (CFD) has an important degree of freedom: the slope of the contract, in dollars per inch of SWE. This is used as a decision variable in the multi-objective optimization, as described in the next section. However, it is useful first to consider the effect of this variable on the performance of the CFD in isolation, without a reserve fund or debt issuance. Let unhedged net revenue refer to the annual hydropower revenue less fixed costs, and hedged net revenue refer to unhedged net revenue plus the net payout from the CFD. Figure 6 shows expected hedged net revenue against the lower 5th percentile of hedged net revenue, for a range of contract slopes from \$0 to \$1.5 million per inch of SWE. A clear tradeoff is evident: as the contract slope increases from zero, the expected hedged net revenues tend to decrease (due to the risk loading paid to the contract seller), while the 5th percentile of hedged net revenues increase (confirming the risk-reducing value of the hedging contract). However, the curve is convex, reaching maximum risk protection at \$0.988 million/inch. As the slope is increased further, the marginal effect of the contract becomes counterproductive, as the large payments due in wet years become a bigger liability than revenue shortfalls in dry years.

To understand how the CFD increases the 5th percentile hedged net revenues (i.e., reduces risk), consider the risk protection-maximizing contract with a slope of \$0.988 million/inch. The effect of this contract is visualized in Figure 7, which shows the mean and 5th-95th percentile band of unhedged and hedged net revenue in different SWE bins. The unhedged revenue distribution shows a clear positive relationship with the SWE index, as expected from the relationship in Figure (3, right). The CFD rotates the distribution

so that cash flows are nearly independent of SWE, although some dependence remains due to the upper cap on payments as well as the slight convexity of the SWE-revenue relationship. Net revenues in low-SWE years, the primary concern from a financial risk perspective, are significantly increased by hedging, while net revenues in high-SWE years are significantly decreased. The far right side of Figure 7 shows the mean and 5th-95th percentile band of the entire net revenue distribution, without consideration of SWE. The unhedged net revenues have a mean of \$10.99 million and a lower 5th percentile of \$-10.84 million. The CFD tends to reduce expected hedged net revenue to \$9.82 million (i.e., the contract costs \$1.17 million/year on average, due to the risk loading charged by the contract seller). The contract also affects upside variability due to the contract payments that must be paid by the utility in wet years, reducing the 95th percentile of hedged net revenues from \$33.78 million to \$22.44 million. However, the 5th percentile of hedged net revenue is increased by \$8.98 million to \$-1.86 million, indicating that this CFD can significantly reduce the risk of extraordinarily large revenue shortfalls.

4.2 Results of Multi-Objective Optimization

If risk minimization were the only decision-making criterion, and if the CFD was the only risk management tool available, then Figure 6 would be the end of our analysis. The ideal contract slope would be the risk-minimizing slope of \$0.988 million/inch. However, decision-makers frequently must navigate tradeoffs between competing objectives, and may utilize a variety of tools to achieve those objectives. In this work, we consider a decision-maker who constructs a portfolio of financial risk management tools by combining a SWE-based contract for differences (CFD) with a reserve fund and short-term debt issuance.

When searching for an optimal risk management strategy, a tradeoff emerges for this decision-maker between the expected annualized cash flow, J^{cash}, and the 95th percentile maximum debt, J^{debt}, objectives. This tradeoff is visualized in Figure 8. The ideal point is shown as a grey star in the lower right corner, where J^{debt} is minimized and J^{cash} is maximized. It is instructive to consider the different strategies employed by the solutions across the Pareto set. In the top right-hand corner of Figure 8 (e.g., near the solution marked A) are solutions that achieve high expected cash flows (i.e., low cost of risk management), but that rely heavily on issuing debt in times of financial stress. These solutions tend to use a relatively small reserve fund and no CFD. By contrast, the bot-

tom left-hand corner of Figure 8 (e.g., near solution C) contains solutions that achieve very low levels of debt, but in return tend to see lower expected cash flows. These solutions tend to utilize a larger reserve fund in addition to a large CFD, and thus are higher cost on average, but only rarely have to rely on debt issuance, since they generally have sufficient protection from the CFD and reserve fund. Lastly, between these two extremes are compromise strategies (e.g., near solution B) that use a smaller CFD in conjunction with a reserve fund in order to achieve intermediate objective values. Table 2 shows the CFD slope, reserve fund limit, and objectives (J^{cash} and J^{debt}) for solutions A, B, and C. Also shown are normalized versions of each objective, $\hat{J}^{cash}$ and $\hat{J}^{debt}$. Each normalized objective is divided by the expected net hydropower revenue, $E[Revenue] * (1 - c)$, where c is the fixed costs as a fraction of expected revenues, 0.914. Expected revenue is \$127.80 million/year, so that the expected net revenue in this case is \$10.99 million/year. The normalized cash flow objective $\hat{J}^{cash}$, then, gives the expected post-management cash flow as a fraction of the expected pre-management net revenue. This is useful in assessing the relative cost of risk management. The normalized debt objective $\hat{J}^{debt}$ gives the debt burden as a multiple of expected pre-management net revenue, which is useful in assessing the utility's ability to pay back the debt. These normalized objectives will allow for a baseline comparison when considering sensitivity to the fixed cost fraction c in Section 4.3.

Although the multi-objective formulation of the search problem focuses on the expected annualized cash flow and the 95th percentile of maximum debt (i.e., the "Ensemble objectives" in Figure 1), it is informative to carefully consider the full distributional performances of the high cash flow (A), low debt (C), and compromise (B) solutions. Figure 9 shows the distributions of annualized cash flow and maximum debt (i.e., the "Simulation objectives" in Figure 1), over the entire ensemble of 20-year simulations, for each of the three highlighted strategies. Despite having the lowest expected annualized cash flows, solution C also has the lowest chance of very low annualized cash flows (e.g., below \$5 million per year over 20 years). It also has a much narrower distribution of debt maxima, which confirms that the solutions with large CFDs and reserve funds are the most risk averse management strategies. In payment for this reduced volatility, solution C has the smallest mean annualized cash flow as well as the smallest chance of significant upside (e.g., above \$15 million per year). As with the ensemble objectives in Fig-

ure 8, B is a compromise solution that is intermediate to solutions A and C in terms of the simulation objective distributions.

The navigation of this tradeoff and selection of a financial risk management policy will depend on decision-maker preferences. This process will depend on personal attitudes, such as risk aversion, as well as a variety of institutional factors, such as the utility's outstanding debt service and credit rating, its ability to raise its customers' rates in order to increase net revenues, and the willingness of its regulators to approve financial contracts like the proposed CFD. These contextual factors affect a decision-maker's navigation of tradeoffs within the Pareto set of a particular SOW. We now turn to the sensitivity analysis, in which we explore how a changing SOW can affect the resulting Pareto set itself.

4.3 Sensitivity to Contextual Financial Parameters

The results presented so far in Sections 4.1 and 4.2 are restricted to the baseline SOW, consisting of financial parameters estimated for SFPUC circa October 2016 (Table 1). In order to explore the effects of the SOW parameters on attainable performance and the optimality of different risk management policies, the multi-objective optimization (MOO), as introduced in Equations 4-6, is repeated for 150 alternative SOWs. Each MOO results in a separate Pareto set, similar the results in Figure 8 for the baseline SOW.

Figure 10 displays the cloud of Pareto-optimal solutions, across the baseline SOW (black) and the 150 alternative SOWs (color). Objective values are normalized by expected net hydropower revenues, as described in Section 4.2. Note that results in Figure 10 are filtered to show only those with $\hat{J}^{debt} < 5$, since a short-term debt load five times larger than expected net revenues would be problematic for many organizations from a credit perspective. However, the full unfiltered results can be found in Supporting Information Figure S7. A tradeoff between expected annualized cash flow ($\hat{J}^{cash}$) and 95th percentile maximum debt load ($\hat{J}^{debt}$) exists across the SOWs. However, the attainable objective values and the severity of the tradeoff varies widely. Solutions in the bottom right-hand corner correspond to states of the world in which risk can be managed effectively at very low cost, while those in the top left-hand corner correspond to states of the world in which very large debt loads may be necessary to meet short-term cash flow shortfalls, even after undertaking relatively expensive risk management actions.

These results suggest that the five contextual financial parameters characterizing the SOW can have a dominant impact on the options available to a decision-maker. A decision-maker operating within the baseline SOW can choose policies attaining $\hat{J}^{debt}$ values between 2.38 and 0.30, with corresponding $\hat{J}^{cash}$ values between 0.99 and 0.88, respectively (Table 2). However, for decision-makers operating in alternative SOWs, the tradeoff and attainable performance can look very different. For example, the arcs of solutions in the upper lefthand quadrant represent states of the world in which all available options are both high cost (i.e., low $\hat{J}^{cash}$) and high debt; the decision-maker is forced to choose from among a set of relatively poor options. It is possible that no options are deemed acceptable to this decision-maker; in this case, the decision-maker may have to resort to alternative tools not considered in this study, such as raising customer rates or building new infrastructure. On the other hand, many SOWs produce Pareto sets that lie entirely in the lower righthand corner, close to the "ideal" point represented by the grey star. The choice of operating policy for these decision-makers may be trivial; all options are very good options and the differences between alternative policies may not be decision-relevant. Lastly, there are many SOWs, including the baseline SOW, in which the Pareto set varies significantly and meaningfully across policies. In these situations, navigation of the tradeoff between $\hat{J}^{cash}$ and $\hat{J}^{debt}$ will depend on decision-maker preferences, as discussed in Section 4.2.

In order to determine which SOW parameters are the most the important determinants of performance, we can plot each objective against each of the parameters defining the SOW. Results for the normalized debt objective, $\hat{J}^{debt}$, and the normalized cash flow objective, $\hat{J}^{cash}$, are shown in Figures 11 and 12, respectively. Again, solutions with $\hat{J}^{debt} < 5$ have been filtered out, but the full results can be seen in Supporting Information Figures S8-S9. For the normalized debt objective, the plot of the fixed cost fraction c (Figure 11, left) shows the clearest sensitivity. For any given c, there are a range of solutions, which can be sorted into strategies using a reserve fund in isolation, a small number of strategies using a CFD in isolation (which will be discussed below), and those using a mixed strategy. The debt objective tends to be higher for strategies using a reserve fund in isolation, relative to mixed strategies, consistent with the tradeoffs seen in Figure 10. The debt objective also tends to increase as the cost fraction c is increased, since larger fixed costs lead to a higher likelihood of negative cash flows. For any given

value of $\hat{J}^{debt}$, a reserve fund-only strategy may be optimal at low c, while the addition of a CFD will become optimal at higher c.

Figure 12 shows the normalized cash flow objective, $\hat{J}^{cash}$, against the contextual parameters defining the SOW. A strong effect is once again evident for the fixed cost fraction c. $\hat{J}^{cash}$ will be equal to one for a strategy in which risk management has zero cost on average (i.e., expected annualized cash flows (post-management) are equal to expected net revenues (pre-management)). For any given c, the reserve fund-only strategies tend to be very low-cost, with $\hat{J}^{cash}$ close to one, while the mixed strategies have higher expected costs. This is consistent with the tradeoff between the cash flow and debt objectives seen in Figure 10. Additionally, the management cost tends to increase as the fixed costs fraction increases: $\hat{J}^{cash} = 60.0\%$ in the most extreme scenarios, indicating that risk management consumes 40% of the utility's expected net hydropower revenues. Figure 11-12 also show that when the fixed cost fraction is greater than 0.943 (compare this to the baseline estimate of $c = 0.914$ for SFPUC as of September 2016), no reserve fund-only strategies are feasible, and no solutions at all are found for fixed cost fractions greater than 0.970. This means that hydropower utilities with very large fixed costs, as a fraction of net hydropower revenues, may be unable to meet their risk management goals using the tools proposed in this study. These constraints are relaxed only slightly if the $\hat{J}^{debt} < 5$ filter is removed (see Supporting Information Figures S8-S9). This highlights the importance of the fixed cost parameter in determining financial outcomes. A utility in this situation would likely need to raise its customer's rates and/or cut costs in order to reduce it's fixed costs fraction to a manageable level.

There are also a small number of strategies that use only a CFD, without a reserve fund. These solutions appear to be lower cost and higher debt in general than the mixed strategies. This is a seemingly unintuitive result because the CFDs are typically higher cost than a reserve fund, due to the risk loading attached by the contract sellers. The sensitivity plots for the market price of risk parameter (λ, Figures 11-12, top right) suggest the reason for this pattern: the CFD-only strategy is only optimal when λ is close to zero, resulting in very inexpensive contracts. The sensitivity plot for λ also suggests that for mixed strategies, there is a trend towards higher-debt and higher-cost solutions when the market price of risk is high. This is to be expected, as the increased cost of the CFD would reduce annualized cash flows and make cash flow shortfalls (and thus debt issuance) more common.

Lastly, the sensitivity plots for the real discount rate (δ, top center) and the real relative interest rates on the reserve fund (Δ_F, bottom center) and debt (Δ_D, bottom right), do not show any clear trends with respect to the debt objective J^{debt} or the cash flow objective J^{cash}. They also do not show any patterns with respect to the optimal choice of reserve fund-only, CFD-only, or mixed strategies. This suggests that the Pareto sets and attainable performances are minimally sensitive to these rates, compared to other contextual parameters in this study.

4.4 Limitations and Future Directions

This study is concerned with relatively short-term financial risk on the order of one year. The contracts last a single year at a time, and no irreversible decisions such as infrastructure investments are considered. A key advantage of such a strategy over managing risk with structural solutions (e.g., increasing the size of a reservoir) is its reversibility and adaptability. Although the optimization is conditioned on 20-year simulation ensembles, the model can be updated and rerun each year as conditions, forecasts, and stakeholder preferences change. Future work will consider this updating strategy explicitly by reformulating the model as a closed loop decision problem, in which model state information is used to dynamically update the decisions at each time step.

Nevertheless, a manager developing a longer-term risk management plan might be able to improve performance by relaxing some of the stationarity assumptions made here. Retail demand is assumed constant over the 20-year simulation, and customer rates, fixed costs, interest rates, and discount rates are assumed constant in inflation-adjusted terms. A utility performing such an analysis might want to include projected (potentially stochastic) change in these factors explicitly. Additionally, the synthetic SWE observations, hydropower generation, and power prices are generated as stationary stochastic processes. However, California power markets have already begun to change in the face of increasing renewable energy penetration (California Independent System Operator, 2018; Zarnikau et al., 2016), a process that will be accelerated in coming years as the state moves towards its ambitious greenhouse gas emission reduction targets (California Energy Commission, 2018; Rheinheimer, Ligare, & Viers, 2012). Prices could also be affected by any significant change in natural gas markets, a major driver of electricity prices in the state (California Independent System Operator, 2018; Zarnikau et al., 2016).

Climate change could affect SWE and hydropower in California through a number of mechanisms (Vicuna & Dracup, 2007). Research on the effect of anthropogenic climate forcing on mean precipitation in California is inconsistent, but interannual variability may increase significantly, leading to more frequent meteorological droughts as well as more frequent extreme precipitation events (Berg & Hall, 2015). Regardless of the trend in precipitation, rising temperatures are expected to increase the co-occurence of low-precipitation events and high-temperature events, leading to more frequent hydrologic droughts (AghaKouchak et al., 2014; Diffenbaugh et al., 2015; Gonzalez et al., 2018; Wehner et al., 2017). In alpine regions, rising temperatures are expected to push snow melt earlier in the year and decrease the proportion of precipitation falling as snow (Hall, Berg, Sun, Walton, & Schwartz, 2017; Kiparsky, Joyce, Purkey, & Young, 2014; McGurk & Hannaford, 2008; Null, Viers, & Mount, 2010; Rheinheimer et al., 2012), and there is evidence that to-date warming has already begun to impact snow hydrology (Berg & Hall, 2017; Fritze, Stewart, & Pebesma, 2011; Fyfe et al., 2017). We find no significant trend in February 1 or April 1 SWE between 1952 and 2016 for this location, likely due to its high elevation, but in the future, or at present for other locations, it would be necessary to account for trends when modeling risk. With respect to SWE-based index contracts such as the proposed CFD, any change in the probability distribution of SWE will alter the distribution of payouts and necessitate a revision of contract terms and pricing. Additionally, the contract buyer will be vulnerable to non-stationarity in the relationship between SWE and hydropower generation (e.g., an increase in reservoir spillage due to faster melting), which will influence the effectiveness of the SWE index for hedging purposes.

Another potential extension of this work would be to supplement the risk management strategies described herein by hedging price risk in the wholesale power markets through derivative contracts on the price of electricity or natural gas (Deng & Oren, 2006). Rather than hedging SWE and power prices independently, it may be more effective to hedge using a composite index that depends on the product of hydrology and power price (Kern, Characklis, & Foster, 2015). In order to model such a hedge, it would be important to accurately capture the complex interplay between hydrology and power prices in California. Spring and summer wholesale power prices tend to decrease in wet years and increase in dry years, all else equal, due to the shift in the supply curve that occurs when reduced hydropower availability causes increased reliance on more expensive sources

(Deng & Oren, 2006; Madani, Guégan, & Uvo, 2014; O'Connell, Voisin, Macknick, & Fu, 2019; Su, Kern, & Characklis, 2017). Therefore, inclusion of pricing information from a market-wide power dispatch model might be expected to introduce a non-linearity into the index-revenue relationship which would dampen overall financial variability. This is an interesting avenue for future research, but beyond the scope of this study.

5 Conclusions

Hydrologic variability poses an important source of financial risk for hydropower-reliant electric utilities. This research develops a methodology for optimizing multi-pronged financial risk management portfolios that combine a reserve fund, short-term debt, and a novel snowpack-based index contract, which differs from typical analyses where each tool is assessed in isolation. In the case of index contracts this ignores the opportunity cost of contract loading; in some situations, the same risk management could be achieved at lower cost using a reserve fund, debt issuance, or some combination of the three. It is also important to measure financial performance over an extended period (e.g., the 20-year simulations used in this work), rather than aggregating independent single-year samples, due to the dynamic and cumulative nature of reserve funds and debt.

The results of this study highlight the importance of institutional context. There is a fundamental tradeoff between cash flows (J^{cash}) and debt levels (J^{debt}), as the strategies that are the lowest cost on average will achieve these cost savings by taking on riskier positions that sometimes require significant debt issuance. Within any particular state of the world (SOW), the navigation of this tradeoff will depend on decision-maker preferences, which are likely to be affected by institutional factors such as the utility's outstanding debt service and credit rating, and its ability to raise its customers' rates in order to increase net revenues. Additionally, the steepness and meaningfulness of the tradeoff between the two objectives will itself be dictated by the contextual factors defining the SOW, such as the ratio of the utility's fixed costs to its average hydropower revenues, and the affordability of index contracts. Interestingly, though, we find that results in this study are not particularly sensitive to real interest rates or the decision-maker's real discount rate.

These results also confirm the potential for snow water equivalent depth (SWE)-based index contracts, such as the proposed capped contract for differences (CFD), to

effectively contribute to hedging the financial risk associated with variability in hydropower production. Snowmelt plays an important hydrologic role across much of western North and South America, northern Europe, and central and northeastern Asia. The methodology and results presented here should be of interest to other power utilities with significant hydropower resources, especially in regions where runoff is primarily dominated by snowmelt. Additionally, SWE-based index contracts may be useful for hedging hydrologic risks in other snowmelt-reliant industries such as municipal water supply and irrigated agriculture. The financial simulation, multi-objective optimization, and sensitivity analysis laid out in this work may also provide a useful framework for the management of environmental financial risks in a variety contexts.

Acknowledgments

Funding for this work was provided by the National Science Foundation (NSF), Innovations at the Nexus of Food-Energy-Water Systems, Track 2 (Award 1639268). The authors would like to thank Alexis Dufour and Darryl Dunn of the San Francisco Public Utilities Commission (SFPUC) for helpful discussion and data provision. The views expressed in this work represent those of the authors and do not necessarily reflect the views or policies of the NSF or SFPUC. All code and data for this project, including figure generation, are available in a live repository (https://github.com/ahamilton144/hamilton-2020-managing-financial-risk-tradeoffs-for-hydropower) and a permanent archive (http://doi.org/10.5281/zenodo.3

References

AghaKouchak, A., Cheng, L., Mazdiyasni, O., & Farahmand, A. (2014). Global warming and changes in risk of concurrent climate extremes: Insights from the 2014 California drought. *Geophysical Research Letters*, *41*, 8847–8852. doi: 10.1002/2014GL062308

Alderman, H., & Haque, T. (2007). *Insurance against covariate shocks: The role of index-based insurance in social protection in low-income countries of Africa.* doi: 10.1596/978-0-8213-7036-0

Anghileri, D., Voisin, N., Castelletti, A., Pianosi, F., Nijssen, B., & Lettenmaier, D. P. (2016). Value of long-term streamflow forecasts to reservoir operations for water supply in snow-dominated river catchments. *Water Resources Research*, *52*, 4209–4225. doi: 10.1002/2015WR017864

Bank, M., & Wiesner, R. (2010). The Use of Weather Derivatives by Small-and Medium- Sized Enterprises: Reasons and Obstacles. *Journal of Small Business and Entrepreneurship*, *23*(4), 581–600. doi: 10.1080/08276331.2010.10593503

Barnett, T. P., Adam, J. C., & Lettenmaier, D. P. (2005). Potential impacts of a warming climate on water availability in snow-dominated regions. *Nature*, *438*, 303–309. doi: 10.1038/nature04141

Baum, R., Characklis, G. W., & Serre, M. L. (2018). Effects of Geographic Diversification on Risk Pooling to Mitigate Drought-Related Financial Losses for Water Utilities. *Water Resources Research*, *54*, 1–19. doi: 10.1002/2017WR021468

Berg, N., & Hall, A. (2015). Increased interannual precipitation extremes over California under climate change. *Journal of Climate*, *28*(16), 6324–6334. doi: 10.1175/JCLI-D-14-00624.1

Berg, N., & Hall, A. (2017). Anthropogenic warming impacts on California snowpack during drought. *Geophysical Research Letters*, *44*, 2511–2518. doi: 10.1002/2016GL072104

Black, F., & Scholes, M. (1973). The Pricing of Options and Corporate Liabilities. *Journal of Political Economy*, *81*(3), 637–654. doi: 10.1086/260062

Blomfield, A., & Plummer, J. (2014). The allocation and documentation of hydrological risk. *Hydropower & Dams*(5), 94–108. doi: 10.1093/rfs/15.4.1283

Brown, C., & Carriquiry, M. (2007). Managing hydroclimatological risk to water supply with option contracts and reservoir index insurance. *Water Resources Research*, *43*, W11423. doi: 10.1029/2007WR006093

Brown, G. W., & Toft, K. B. (2002). How Firms Should Hedge. *The Review of Financial Studies*, *15*(4), 1283–1324.

Bureau of Labor Statistics. (2019). *CIP-All Urban Consumers.* Retrieved from `https://data.bls.gov/cgi-bin/surveymost`

California Data Exchange Center. (2018). *Snow Query: Dana Meadows.* Retrieved from `http://cdec.water.ca.gov/cgi-progs/snowQuery?course_num=dan&month=%28All%29&start_date=&end_date=&csv_mode=Y&data_wish=Raw+Data`

California Energy Commission. (2018). *Total System Electric Generation.* Retrieved from `https://www.energy.ca.gov/almanac/electricity_data/total_system_power.html`

California Independent System Operator. (2018). *2017 Annual Report on Market Issues and Performance* (Tech. Rep.). California Independent System Operator. Retrieved from `http://www.caiso.com/Documents/2017AnnualReportonMarketIssuesandPerformance.pdf`

Carriquiry, M. A., & Osgood, D. E. (2012). Index Insurance, Probabilistic Climate Forecasts, and Production. *Journal of Risk and Insurance*, *79*(1), 287–300. doi: 10.1111/j.1539-6975.2011.01422.x

Chicago Mercantile Exchange Group. (2007). *Weather Futures and Options* (Tech. Rep.). Chicago Mercantile Exchange Group. Retrieved from `www.cmegroup.com/weather.`

Chicago Mercantile Exchange Group. (2014). *Snowfall Futures and Options* (Tech. Rep.). Chicago Mercantile Exchange Group. Retrieved from `www.cmegroup.com/snowfall.`

Coello Coello, C. A., Lamont, G. B., & Van Veldhuizen, D. A. (2007). *Evolutionary Algorithms for Solving Multi-Objective Problems* (2nd ed.; D. E. Goldberg & J. R. Koza, Eds.). Springer Science+Business Media, LLC. doi: 10.1046/j.1365-2672.2000.00969.x

Conradt, S., Finger, R., & Bokusheva, R. (2015). Tailored to the extremes: Quantile regression for index-based insurance contract design. *Agricultural Economics*, *46*, 537–547. doi: 10.1111/agec.12180

Cyr, D., & Kusy, M. (2007). Canadian Ice Wine Production: A Case for the Use of Weather Derivatives. *Journal of Wine Economics*, *2*(2), 145–167. doi: 10.1017/s1931436100000407

Denaro, S., Anghileri, D., Giuliani, M., & Castelletti, A. (2017). Informing the operations of water reservoirs over multiple temporal scales by direct use of hydro-meteorological data. *Advances in Water Resources*, *103*, 51–63. doi: 10.1016/j.advwatres.2017.02.012

Denaro, S., Castelletti, A., Giuliani, M., & Characklis, G. W. (2018). Fostering cooperation in power asymmetrical water systems by the use of direct release rules and index-based insurance schemes. *Advances in Water Resources*, *115*, 301–314. doi: 10.1016/j.advwatres.2017.09.021

Deng, S., & Oren, S. (2006). Electricity derivatives and risk management. *Energy*, *31*(6), 940–953. doi: 10.1016/j.energy.2005.02.015

Diffenbaugh, N. S., Swain, D. L., & Touma, D. (2015). Anthropogenic warming has increased drought risk in California. *Proceedings of the National Academy of Sciences*, *112*(13), 3931–3936. doi: 10.1073/pnas.1422385112

Ellithorpe, D., & Putnam, S. (2000). Weather derivatives and their implications for power markets. *Journal of Risk Finance*, *1*(2), 19–28. doi: 10.1108/eb043442

Foster, B. T., Kern, J. D., & Characklis, G. W. (2015). Mitigating hydrologic financial risk in hydropower generation using index-based financial instruments. *Water Resources and Economics*, *10*, 45–67. doi: 10.1016/j.wre.2015.04.001

Frees, E. W., & Valdez, E. A. (1998). Understanding relationships using copulas. *North American Actuarial Journal*, *2*(1), 1–25. doi: 10.1080/10920277.1998.10595667

Fritze, H., Stewart, I. T., & Pebesma, E. (2011). Shifts in Western North American Snowmelt Runoff Regimes for the Recent Warm Decades. *Journal of Hydrometeorology*, *12*(5), 989–1006. doi: 10.1175/2011jhm1360.1

Froot, K., Scharfstein, D., & Stein, J. (1993). Risk Management: Coordinating Corporate Investment and Financing Policies. *The Journal of Finance*, *48*(5), 1629–1648. doi: 10.1111/j.1540-6261.1993.tb05123.x

Fyfe, J. C., Derksen, C., Mudryk, L., Flato, G. M., Santer, B. D., Swart, N. C., ... Jiao, Y. (2017). Large near-term projected snowpack loss over the western United States. *Nature Communications*, *8*, 1–7. doi: 10.1038/ncomms14996

Genest, C., & Favre, A.-C. (2007). Everything You Always Wanted to Know about Copula Modeling but Were Afraid to Ask. *Journal of Hydrologic Engineering*, *12*(4), 347–368. doi: 10.1061/(asce)1084-0699(2007)12:4(347)

Genest, C., Favre, A. C., Béliveau, J., & Jacques, C. (2007). Metaelliptical copulas and their use in frequency analysis of multivariate hydrological data. *Water Resources Research*, *43*(9), 1–12. doi: 10.1029/2006WR005275

Gleick, P. H. (2017). *Impacts of California's Five-Year (2012-2016) Drought on Hydroelectricity Generation* (Tech. Rep.). Pacific Institute.

Gonzalez, P., Garfin, G., Breshears, D., Brooks, K., Brown, H., Elias, E., ... Udall, B. (2018). Southwest. In D. Reidmiller et al. (Eds.), *Impacts, risks, and adaptation in the united states: Fourth national climate assessment, volume ii* (p. 1101–1184). Washington, DC, USA: U.S. Global Change Research Program. doi: 10.7930/NCA4.2018.CH25

Hadka, D. (2015). *MOEA Framework - A Free and Open Source Java Framework for Multiobjective Optimization.* Retrieved from `http://moeaframework.org`

Hadka, D., & Reed, P. (2013). Borg: An auto-adaptive many-objective evolutionary computing framework. *Evolutionary Computation*, *21*(2), 231–259. doi: 10.1162/EVCO{_}a{_}00075

Hall, A., Berg, N., Sun, F., Walton, D., & Schwartz, M. (2017). Significant and Inevitable End-of-Twenty-First-Century Advances in Surface Runoff Timing in California's Sierra Nevada. *Journal of Hydrometeorology*, *18*(12), 3181–3197. doi: 10.1175/jhm-d-16-0257.1

Hull, J. C. (2009). *Options, Futures, and Other Derivatives* (8th ed.). Boston, MA: Prentice Hall.

Jewson, S., Brix, A., & Ziehmann, C. (2005). *Weather derivative valuation: The meteorological, statistical, financial and mathematical foundations.* Cambridge, UK: Cambridge University Press. doi: 10.1017/CBO9780511493348

Kapnick, S. B., Yang, X., Vecchi, G. A., Delworth, T. L., Gudgel, R., Malyshev, S., ... Dunne, T. (2018). Potential for western US seasonal snowpack prediction. *PNAS*, *115*(6), 1180–1185. doi: 10.1073/pnas.1716760115

Kasprzyk, J. R., Reed, P. M., Characklis, G. W., & Kirsch, B. R. (2012). Many-objective de Novo water supply portfolio planning under deep uncertainty. *Environmental Modelling and Software*, *34*, 87–104. doi: 10.1016/j.envsoft.2011.04.003

Kern, J. D., Characklis, G. W., & Foster, B. T. (2015). Natural gas price uncertainty and the cost-effectiveness of hedging against low hydropower revenues caused by drought. *Water Resources Research*, *51*, 2412–2427. doi: 10.1002/2014WR016533

Kiparsky, M., Joyce, B., Purkey, D., & Young, C. (2014). Potential impacts of climate warming on water supply reliability in the Tuolumne and Merced River Basins, California. *PLoS ONE*, *9*(1), e84946. doi: 10.1371/journal.pone.0084946

Larson, W. M., Freedman, P. L., Passinsky, V., Grubb, E., & Adriaens, P. (2012). Mitigating corporate water risk: Financial market tools and supply management strategies. *Water Alternatives*, *5*(3), 582–602.

Lund, J., Medellin-Azuara, J., Durand, J., & Stone, K. (2018). Lessons from Cal-

ifornia's 2012-2016 Drought. *Journal of Water Resources Planning and Management*, *144*(10), 04018067. doi: 10.1061/(ASCE)WR.1943-5452.0000984

Madani, K., Guégan, M., & Uvo, C. B. (2014). Climate change impacts on high-elevation hydroelectricity in California. *Journal of Hydrology*, *510*, 153–163. doi: 10.1016/j.jhydrol.2013.12.001

Maier, H. R., Kapelan, Z., Kasprzyk, J., Kollat, J., Matott, L. S., Cunha, M. C., ... Reed, P. M. (2014). Evolutionary algorithms and other metaheuristics in water resources: Current status, research challenges and future directions. *Environmental Modelling and Software*, *62*, 271–299. doi: 10.1016/j.envsoft.2014.09.013

Manfredo, M. R., & Richards, T. J. (2009). Hedging with weather derivatives: A role for options in reducing basis risk. *Applied Financial Economics*, *19*(2), 87–97. doi: 10.1080/09603100701765166

Margulis, S. A., Cortés, G., Girotto, M., & Durand, M. (2016). A Landsat-Era Sierra Nevada Snow Reanalysis (1985–2015). *Journal of Hydrometeorology*, *17*, 203–221. doi: 10.1175/JHM-D-15-0177.1

McGurk, B., & Hannaford, M. (2008). Near-term global warming effect on Hetch Hetchy inflow. In *Proc. 76th western snow conference* (pp. 85–90).

Meyer, E. S., Characklis, G. W., & Brown, C. (2017). Evaluating financial risk management strategies under climate change for hydropower producers on the Great Lakes. *Water Resources Research*, *53*(3), 2114–2132. doi: 10.1002/2016WR019889

Meyer, E. S., Characklis, G. W., Brown, C., & Moody, P. (2016). Hedging the financial risk from water scarcity for Great Lakes shipping. *Water Resources Research*, *52*(1), 227–245. doi: 10.1002/2015WR017855

Moody's Investors Service. (2011). *Rating Methodology: U.S. Public Power Electric Utilities with Generation Ownership Exposure* (Tech. Rep.).

Moody's Investors Service. (2019). *Bonneville Power Administration , OR: Credit Update Following Rating Affirmation and Change in Outlook to Negative* (Tech. Rep.).

Nadolnyak, D., & Vedenov, D. (2013). Information Value of Climate Forecasts for Rainfall Index Insurance. *Journal of Agricultural and Applied Economics*, *45*(1), 109–124. doi: 10.1017/S1074070800004612

Nicklow, J., Reed, P., Savic, D., Dessalegne, T., Harrell, L., Chan-Hilton, A., ... Zechman, E. (2010). State of the Art for Genetic Algorithms and Beyond in Water Resources Planning and Management. *Journal of Water Resources Planning and Management*, *136*(4), 412–432. doi: 10.1061/ASCEWR.1943-5452.0000053

Nielsen, C. (2012). *A Market for Snow: How Businesses Use Futures to Prepare for Winter - OpenMarketsOpenMarkets.* Retrieved from `http://openmarkets.cmegroup.com/4967/a-market-for-snow-how-some-businesses-use-futures-to-prepare-for-winter`

Null, S. E., Viers, J. H., & Mount, J. F. (2010). Hydrologic response and watershed sensitivity to climate warming in California's Sierra Nevada. *PLoS ONE*, *5*(4), e9932. doi: 10.1371/journal.pone.0009932

O'Connell, M., Voisin, N., Macknick, J., & Fu, T. (2019). Sensitivity of Western U.S. power system dynamics to droughts compounded with fuel price variability. *Applied Energy*, *247*, 745–754. doi: 10.1016/j.apenergy.2019.01.156

Oum, Y., Oren, S., & Deng, S. (2006). Hedging quantity risks with standard power options in a competitive wholesale electricity market. *Naval Research Logistics*, *53*(7), 697–712. doi: 10.1002/nav.20184

Quinn, J. D., Reed, P. M., Giuliani, M., & Castelletti, A. (2017). Rival framings: A framework for discovering how problem formulation uncertainties shape risk management trade-offs in water resources systems. *Water Resources Research*, *53*(8), 7208–7233. doi: 10.1002/2017WR020524

Reed, P. M., Hadka, D., Herman, J. D., Kasprzyk, J. R., & Kollat, J. B. (2013). Evolutionary multiobjective optimization in water resources: The past, present, and future. *Advances in Water Resources*, *51*, 438–456. doi: 10.1016/j.advwatres.2012.01.005

Rheinheimer, D. E., Ligare, S. T., & Viers, J. H. (2012). *Water and Energy Sector Vulnerability to Climate Warming in the Sierra Nevada: Simulating the Regulated Rivers of California's West Slope Sierra Nevada* (Tech. Rep.). California Energy Commission California Climate Change Center.

San Francisco Public Utilities Commission. (2015). *Hetch Hetchy Water & Power, Financial Statements, June 30, 2015 and 2014* (Tech. Rep.).

San Francisco Public Utilities Commission. (2016). *Comprehensive Annual Financial*

Report, Fiscal Years Ended June 30, 2016 and 2015 (Tech. Rep.).

San Francisco Public Utilities Commission. (2018). *Hydropower generation dataset.* Retrieved from https://github.com/ahamilton144/hamilton-2020-managing-financial-risk-tradeoffs-for-hydropower/blob/master/data/downloaded_inputs/SFPUC_Combined_Public.xlsx

Shukla, S., & Lettenmaier, D. P. (2011). Seasonal hydrologic prediction in the United States: Understanding the role of initial hydrologic conditions and seasonal climate forecast skill. *Hydrology and Earth System Sciences*, *15*(11), 3529–3538. doi: 10.5194/hess-15-3529-2011

Sklar, A. (1973). Random Variables, Joint Distribution Functions, and Copulas. *Kybernetika*, *9*(6), 449–460.

Su, Y., Kern, J. D., & Characklis, G. W. (2017). The impact of wind power growth and hydrological uncertainty on financial losses from oversupply events in hydropower-dominated systems. *Applied Energy*, *194*, 172–183. doi: 10.1016/j.apenergy.2017.02.067

The Vanguard Group. (2019). *VMFXX - Vanguard Federal Money Market Fund — Vanguard.* Retrieved from https://investor.vanguard.com/mutual-funds/profile/performance/vmfxx/cumulative-returns

United States Department of Agriculture Risk Management Agency. (2017). *Pasture Rangeland Forage Pilot Insurance Program.* Retrieved from https://www.rma.usda.gov/en/Fact-Sheets/National-Fact-Sheets/Pasture-Rangeland-Forage-Pilot-Insurance-Program

United States Department of the Treasury. (2019). *Daily Treasury Yield Curve Rates.* Retrieved from https://www.treasury.gov/resource-center/data-chart-center/interest-rates/pages/TextView.aspx?data=yieldYear&year=2016

United States Energy Information Administration. (2017). *Wholesale Electricity and Natural Gas Market Data.* Retrieved from https://www.eia.gov/electricity/wholesale/

Vedenov, D. V., & Barnett, B. J. (2004). Efficiency of weather derivatives as primary crop insurance instruments. *Journal of Agricultural and Resource Economics*, *29*(3), 387–403.

Vicuna, S., & Dracup, J. A. (2007). The evolution of climate change impact studies

on hydrology and water resources in California. *Climatic Change*, *82*, 327–350. doi: 10.1007/s10584-006-9207-2

Wang, S. S. (1999). "Understanding Relationships Using Copulas," Edward Frees and Emiliano Valdez, January 1998. *North American Actuarial Journal*, *3*(1), 137–142. doi: 10.1080/10920277.1999.10595785

Wang, S. S. (2002). A Universal Framework for Pricing Financial and Insurance Risks. *ASTIN BULLETIN*, *32*(2), 213–234. doi: 10.2143/AST.32.2.1027

Wehner, M., Arnold, J., Knutson, T., Kunkel, K., & LeGrande, A. (2017). Droughts, Floods, and Wildfires. In D. Wuebbles, D. Fahey, K. Hibbard, D. Dokken, B. Stewart, & T. Maycock (Eds.), *Climate science special report: Fourth national climate assessment, volume i* (pp. 231–256). Washington, DC, USA: U.S. Global Change Research Program. doi: 10.7930/J0CJ8BNN

Woodward, J. D., & García, P. (2008). Basis risk and weather hedging effectiveness. *Agricultural Finance Review*, *68*(1), 99–117. doi: 10.1108/00214660880001221

Wrzesien, M. L., Durand, M. T., Pavelsky, T. M., Howat, I. M., Margulis, S. A., & Huning, L. S. (2017). Comparison of Methods to Estimate Snow Water Equivalent at the Mountain Range Scale: A Case Study of the California Sierra Nevada. *Journal of Hydrometeorology*, *18*, 1101–1119. doi: 10.1175/JHM-D-16-0246.1

Young, V. R. (2004, 9). Premium Principles. *Encyclopedia of Actuarial Science*. Retrieved from `http://doi.wiley.com/10.1002/9780470012505.tap027` doi: 10.1002/9780470012505.tap027

Zarnikau, J., Moore, J., Ho, T., Chawla, K., Schneiderman, B., Woo, C., ... Olson, A. (2016). Merit-order effects of renewable energy and price divergence in California's day-ahead and real-time electricity markets. *Energy Policy*, *92*, 299–312. doi: 10.1016/j.enpol.2016.02.023

Zatarain Salazar, J., Reed, P. M., Quinn, J. D., Giuliani, M., & Castelletti, A. (2017). Balancing exploration, uncertainty and computational demands in many objective reservoir optimization. *Advances in Water Resources*, *109*, 196–210. doi: 10.1016/j.advwatres.2017.09.014

Zeff, H. B., & Characklis, G. W. (2013). Managing water utility financial risks through third-party index insurance contracts. *Water Resources Research*, *49*(4939-4951). doi: 10.1002/wrcr.20364

Zheng, Z., Molotch, N. P., Oroza, C. A., Conklin, M. H., & Bales, R. C. (2018). Spatial snow water equivalent estimation for mountainous areas using wireless-sensor networks and remote-sensing products. *Remote Sensing of Environment*, *215*, 44–56. doi: 10.1016/j.rse.2018.05.029

6 Tables

Table 1. Estimates for contextual financial parameters defining the state of the world (SOW) in the baseline case, as well as sampling bounds for these parameters in the sensitivity analysis. Discount rate and interest rates are real (i.e. net of inflation), and interest rates are relative to the discount rate, as described in Section 3.9

Parameter	Symbol	Estimate	Min	Max
Fixed cost fraction (unitless)	c	0.914	0.85	1.0
Real discount rate (%/year)	δ	0.4	0.0	5.0
Real (relative) interest rate for fund (%/year)	Δ_F	-1.73	-2.0	0.0
Real (relative) interest rate for debt (%/year)	Δ_D	1.0	0.0	5.0
Market price of risk (unitless)	λ	0.25	0.0	0.5

Table 2. CFD slope and reserve fund limit for selected solutions shown in Figure 8, along with the expected annualized cash flow J^{cash}, 95th percentile maximum debt J^{debt}, and their normalized values $\hat{J}^{cash}$ and $\hat{J}^{debt}$.

Solution	CFD slope ($M/inch)	Reserve fund limit ($M)	J^{cash} ($M/year)	$\hat{J}^{cash}$ (unitless)	J^{debt} ($M)	$\hat{J}^{debt}$ (unitless)
High cash flow (A)	0.00	6.45	10.90	0.99	27.35	2.49
Compromise (B)	0.32	16.05	10.37	0.94	11.25	1.02
Low debt (C)	0.96	19.64	9.53	0.87	2.54	0.23

1291 # 7 Figures

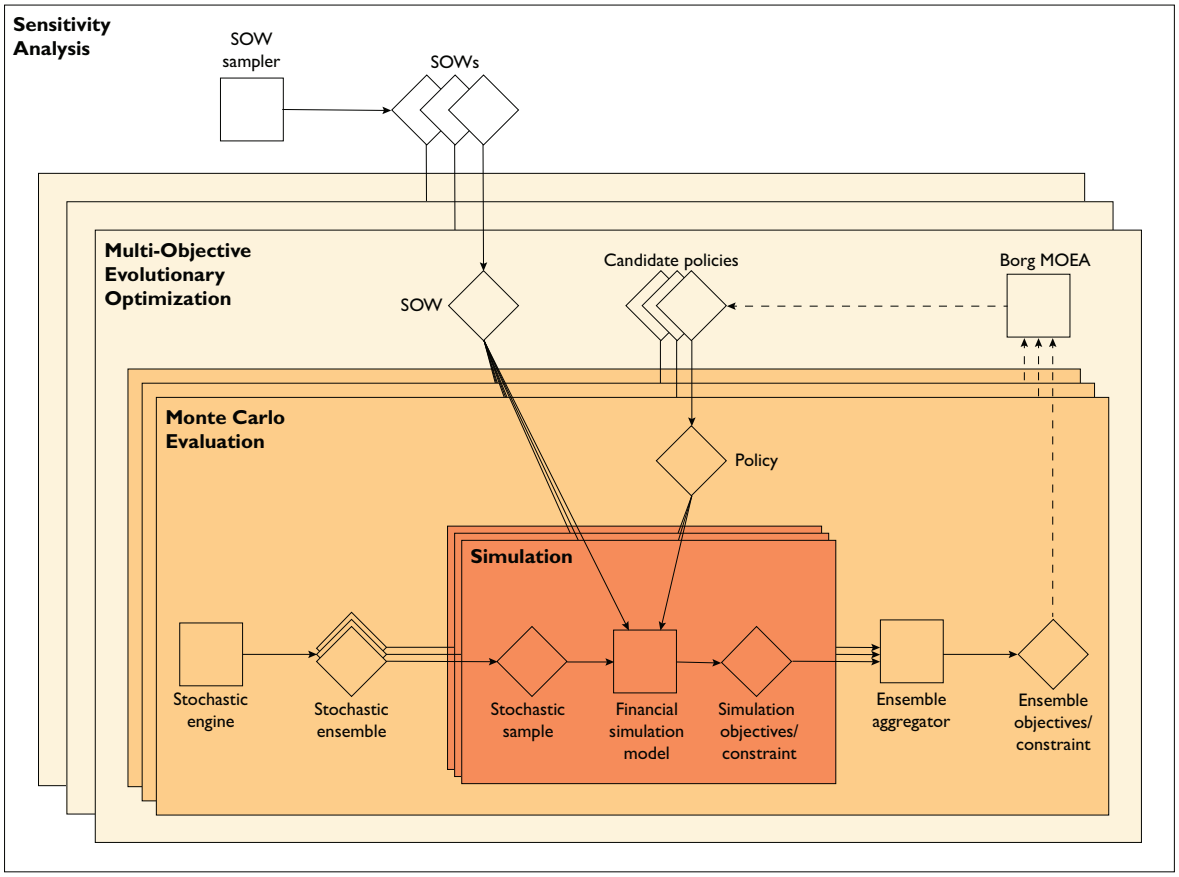

Figure 1. Schematic showing overall workflow for this study. Squares represent processes and diamonds represent inputs/outputs. Dashed arrows show the feedback loop for the Borg Multi-Objective Evolutionary Algorithm (MOEA), where the objective and constraint values for prior candidate policy evaluations are used to generate new candidate policies for evaluation.

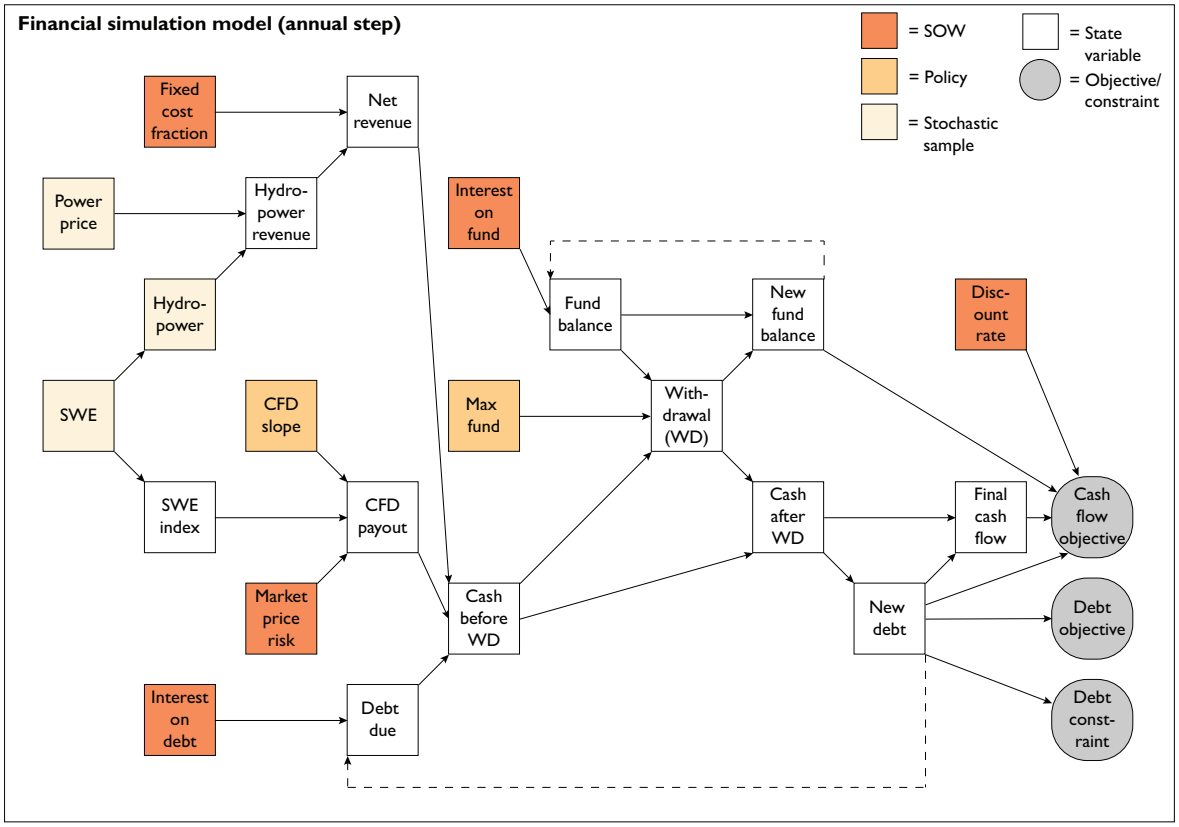

Figure 2. Detailed representation of financial simulation model (as seen in Figure 1) at an annual time step. Arrows denote information flows for the financial operations each year, and dashed lines show information feedbacks from the prior year. A withdrawal (WD) can either be a true withdrawal from (positive values) or a deposit to (negative values) the reserve fund.

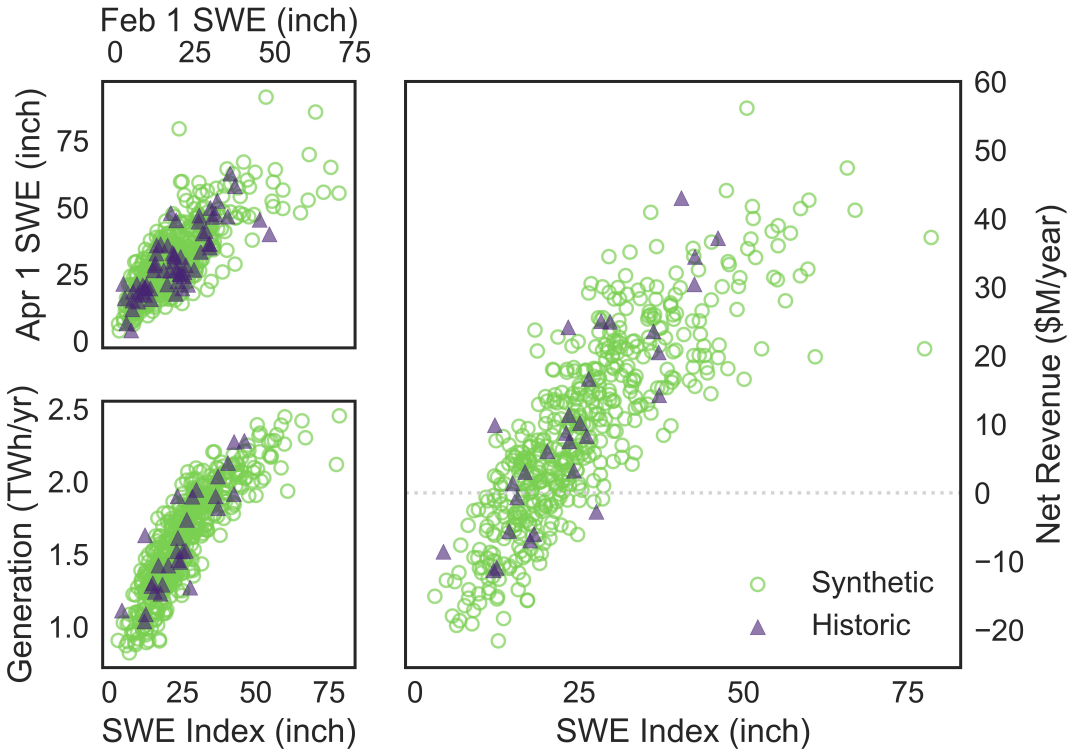

Figure 3. Distribution of historic and synthetic data points for snow water equivalent depth (SWE) on February 1 vs. April 1 (top left), SWE index vs. annual hydropower generation (bottom left), and SWE index vs. annual hydropower net revenue (right). Each plot shows a sample of 500 synthetic data points, while the historic datasets contain 64, 29, and 29 observations, respectively.

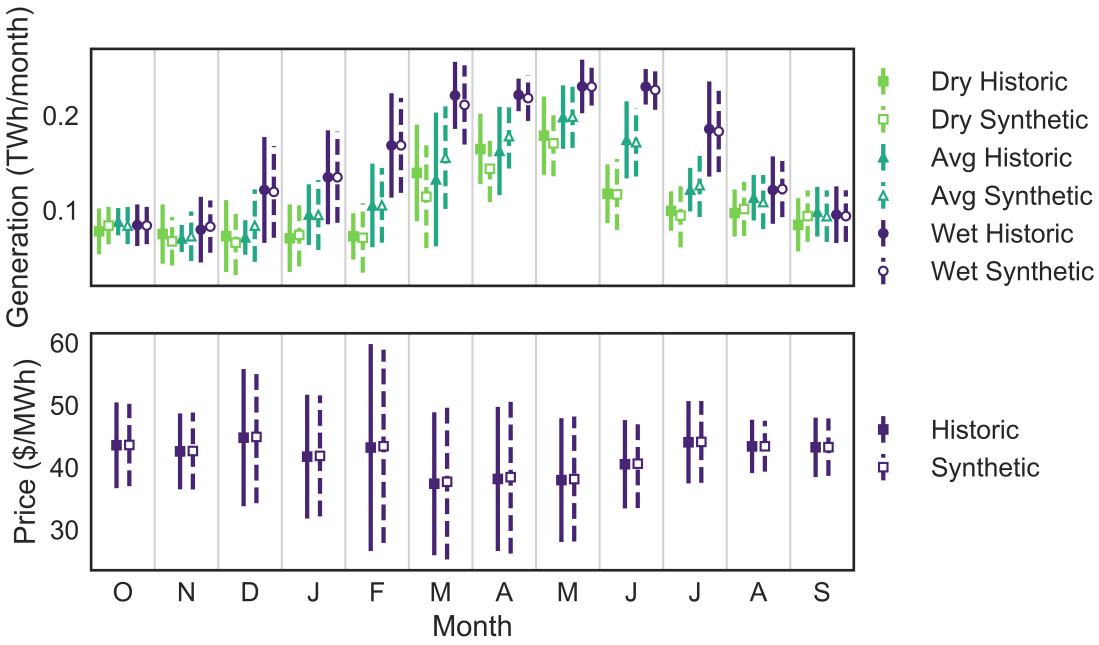

Figure 4. (top) Monthly hydropower generation in historical and synthetic datasets. Results are split into thirds based on the SWE index: dry, average, and wet. (b) Monthly average wholesale power prices in historical and synthetic datasets. Markers show means and error bars show standard deviations.

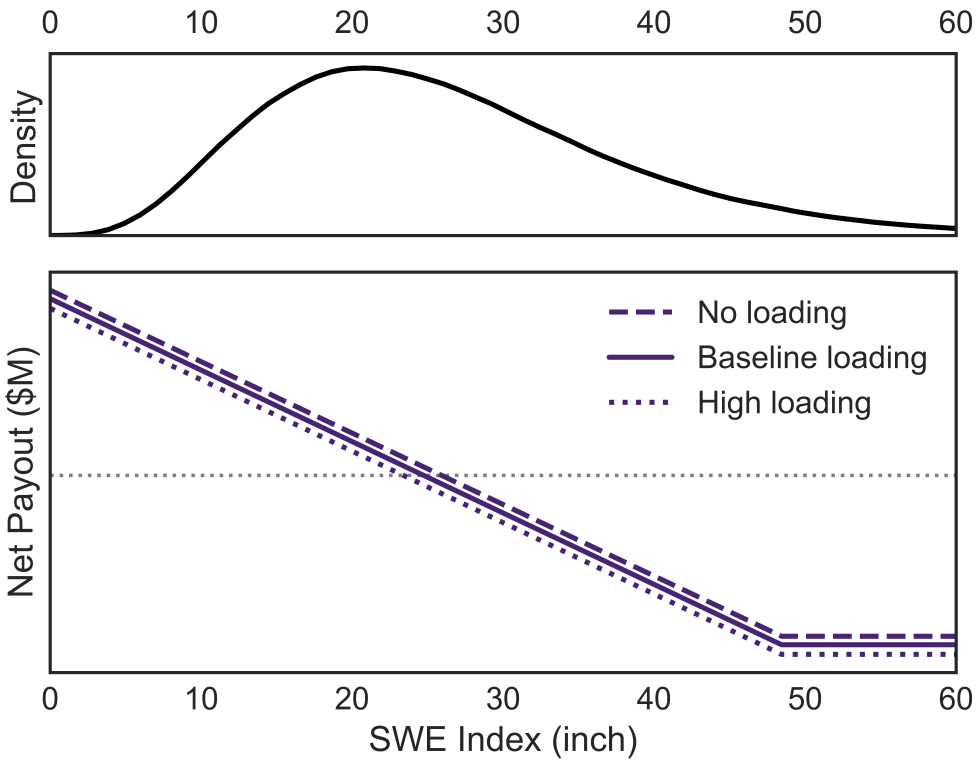

Figure 5. (top) Probability density for SWE index, a weighted average of February 1 and April 1 observations. (bottom) Net payout of capped contract for differences (CFD). Three market prices of risk are shown: no loading ($\lambda = 0$), baseline loading ($\lambda = 0.25$), and high loading ($\lambda = 0.5$).

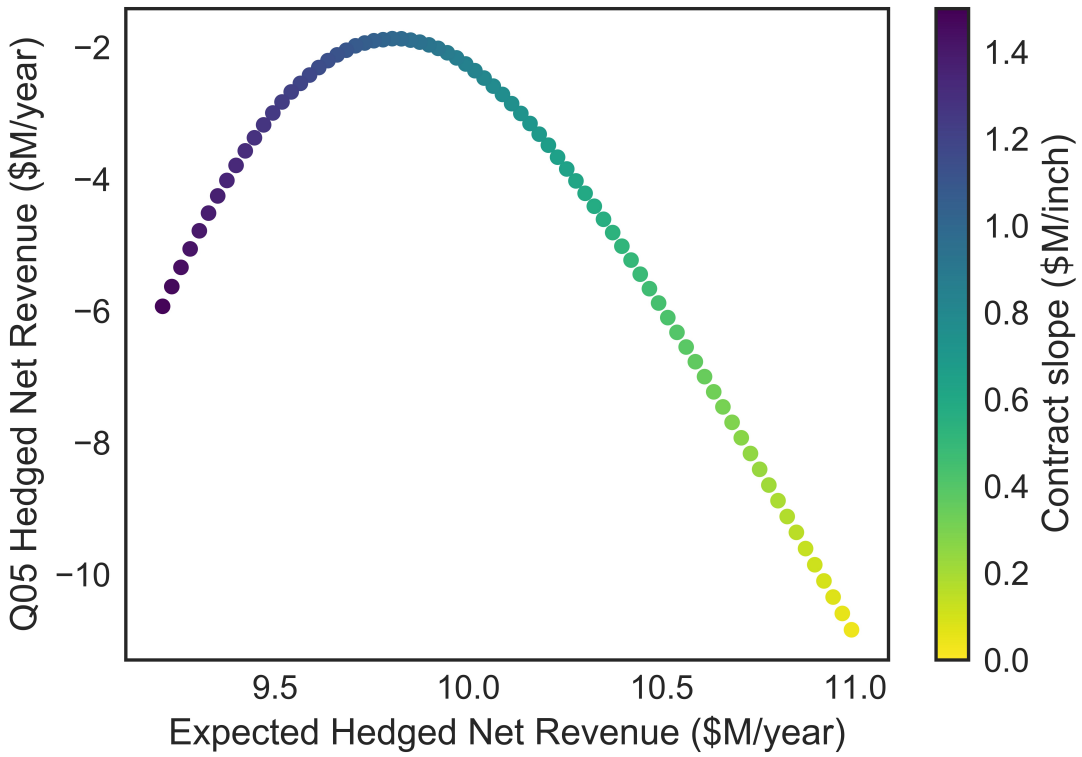

Figure 6. Effect of CFD slope (in $M/inch SWE) on mean and lower 5th percentile of hedged net hydropower revenues.

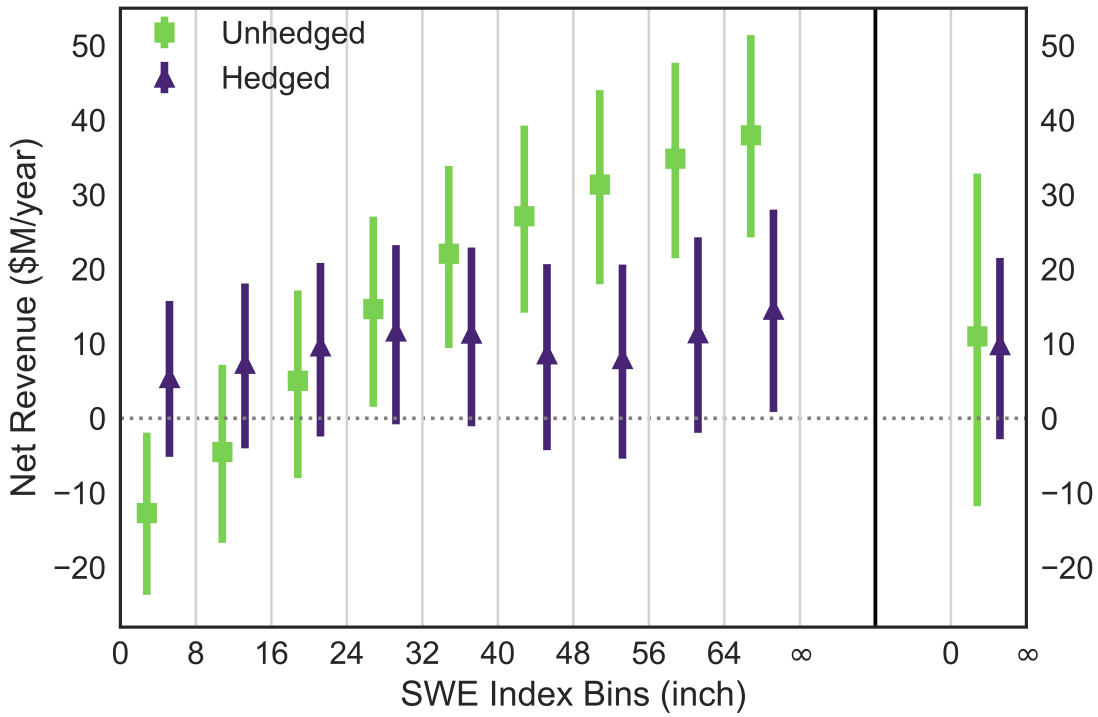

Figure 7. Distribution of net hydropower revenues as a function of SWE index, both before ("Unhedged") and after ("Hedged") adding the net payout from the CFD. Markers show means and lines show the 5th-95th percentile band. Furthest right bin shows the statistics over all SWE values. Contract slope set to $1.033 million per inch SWE, based on maximum of curve in Figure 6.

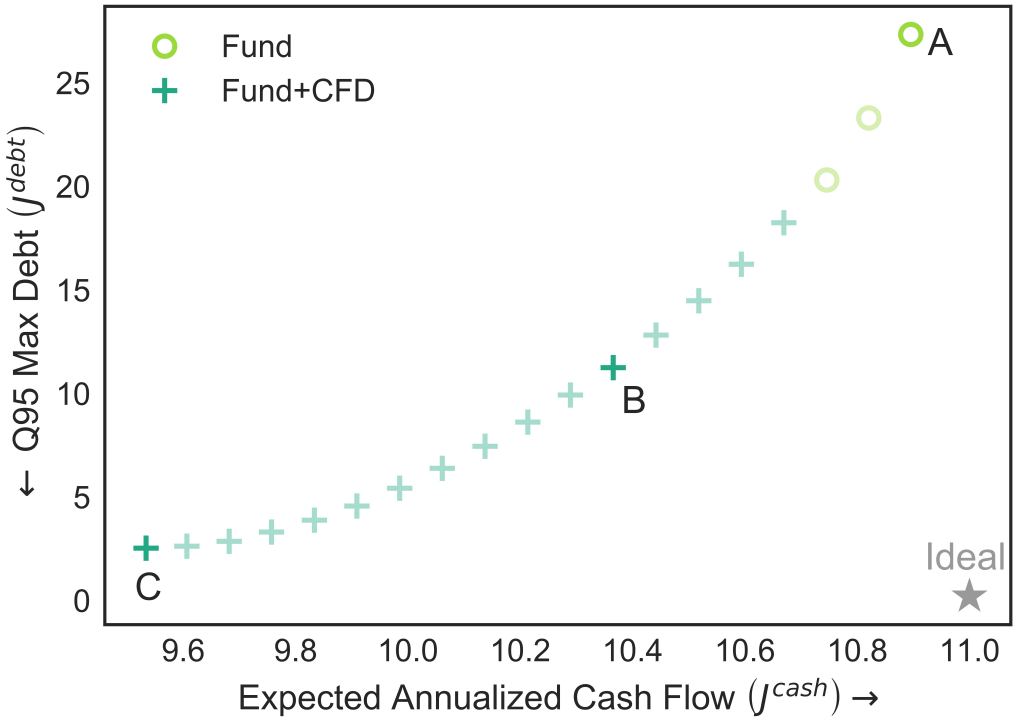

Figure 8. Approximate Pareto-optimal set of solutions for two-objective optimization. The grey star signifies the ideal combination of a maximized expected annualized cash flow (J^{cash}) and minimized 95th percentile maximum debt (J^{debt}). The tradeoff is demonstrated by three highlighted solutions: a high cash flow strategy (A), a low debt strategy (C), and a compromise strategy (B).

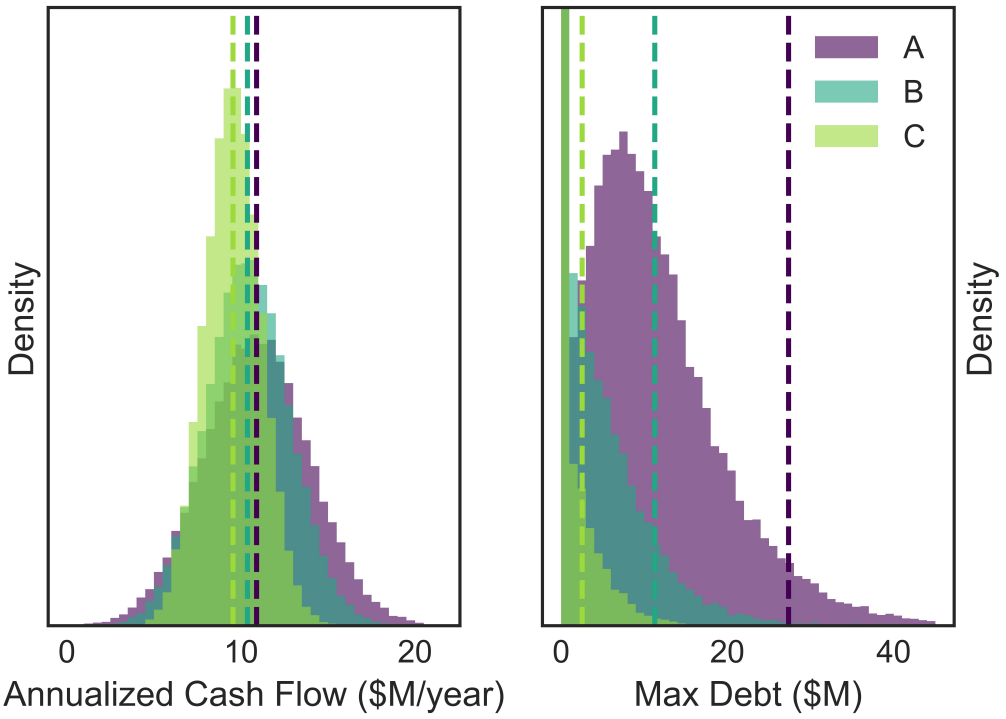

Figure 9. Distribution of annualized cash flow (left) and maximum debt (right) over 20 years for the three strategies highlighted in Figure 8: a high cash flow strategy (A), a low debt strategy (C), and a compromise strategy (B). Dashed lines show the ensemble objectives used in the optimization: expectation of annualized cash flow (left) and 95th percentile of maximum debt (right).

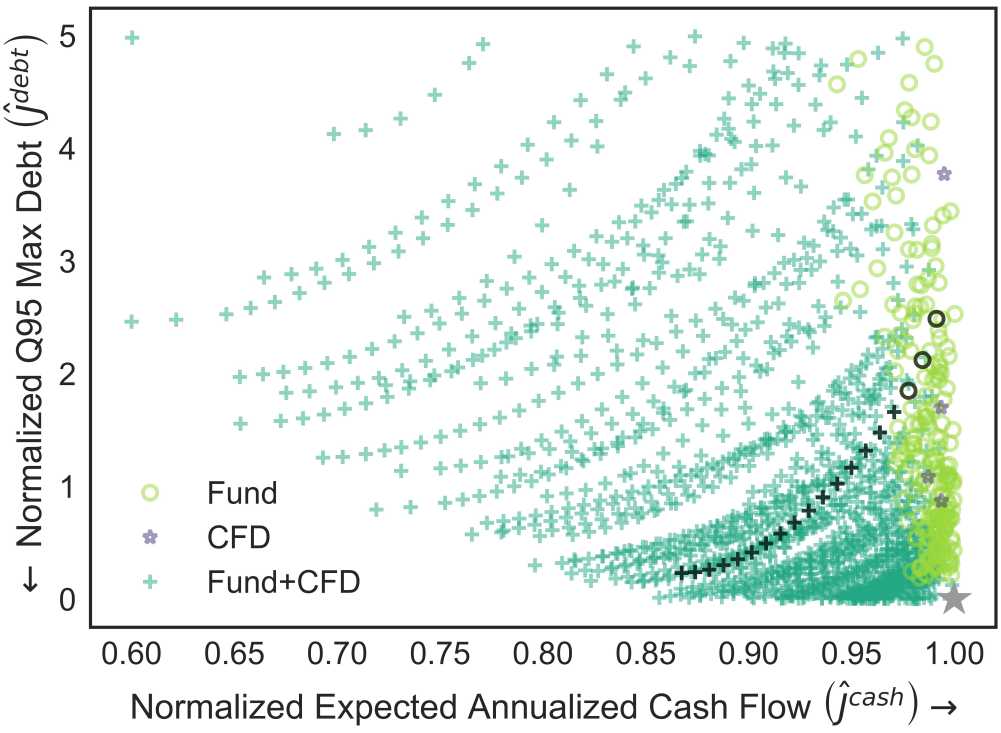

Figure 10. Set of possible tradeoffs between normalized debt objective ($\hat{J}^{debt}$) and normalized cash flow objective ($\hat{J}^{cash}$), after 150 samples of five contextual financial parameters defining the state of the world (SOW). The optimal management strategy falls into three categories, as seen in the legend: reserve fund only, CFD only, or both. Results for baseline 2016 parameter estimates (as seen in Figure 8 are shown in black. The grey star signifies the ideal combination of a maximized $\hat{J}^{cash}$) and minimized $\hat{J}^{debt}$.

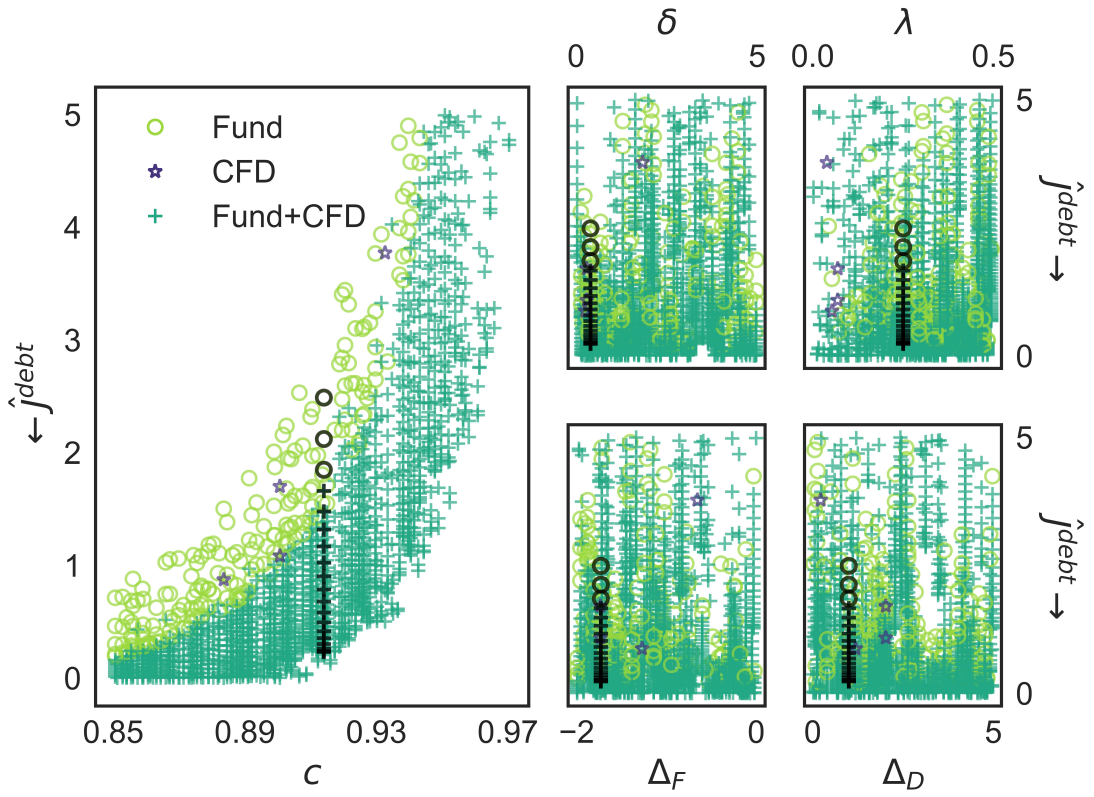

Figure 11. Sensitivity of optimal risk management strategy and normalized debt objective ($\hat{J}^{debt}$) to contextual parameters defining the state of the world (SOW): cost fraction (c, left), discount rate relative to inflation (δ, top center), market price of risk (λ, top right), interest rate markdown on reserve fund relative to discount rate (Δ_F, bottom center), and interest rate markup on debt relative to discount rate (Δ_D, bottom right). Results for baseline 2016 parameter estimates (as seen in Figure 8) are shown in black.

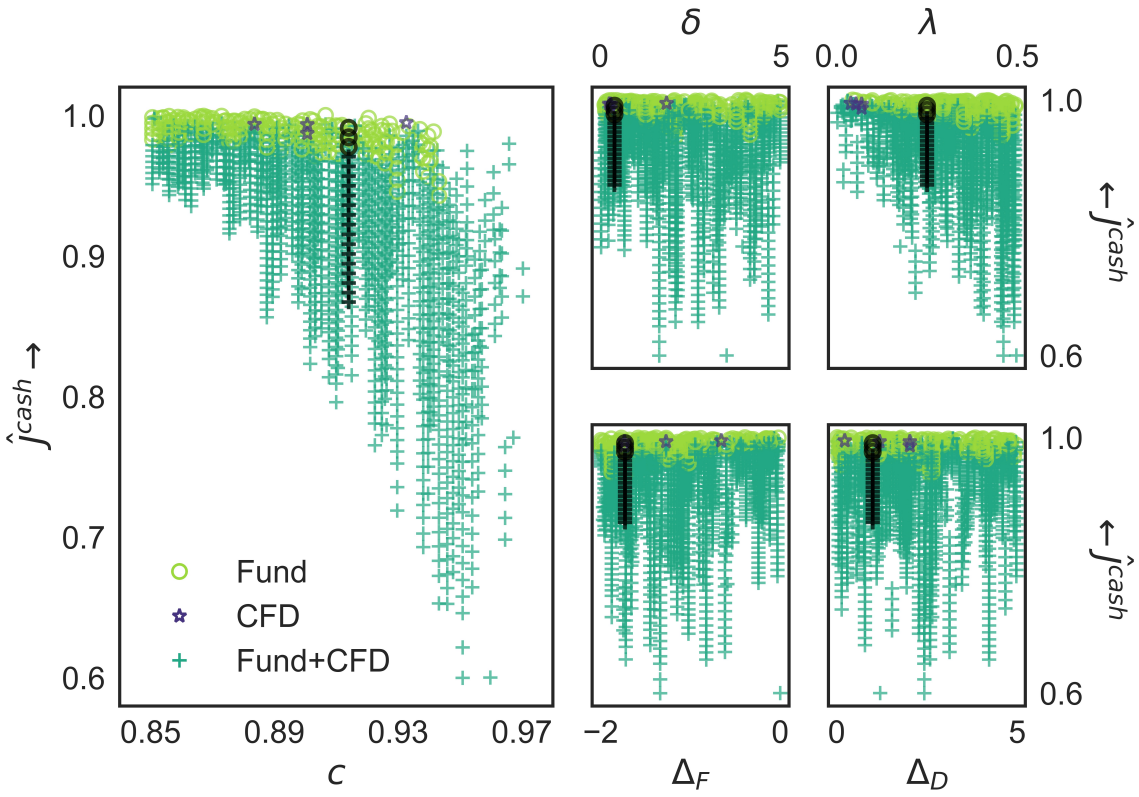

Figure 12. Sensitivity of optimal risk management strategy and normalized cash flow objective ($\hat{J}^{cash}$) to five contextual financial parameters defining the state of the world (SOW): cost fraction (c, left), discount rate relative to inflation (δ, top center), market price of risk (λ, top right), interest rate markdown on reserve fund relative to discount rate (Δ_F, bottom center), and interest rate markup on debt relative to discount rate (Δ_D, bottom right). Results for baseline 2016 parameter estimates (as seen in Figure 8) are shown in black.